JOURNAL OF PROPULSION AND POWER
Vol. 33, No. 3, May–June 2017



# Recommended Practice for Use of Emissive Probes in Electric Propulsion Testing

J. P. Sheehan*
*University of Michigan, Ann Arbor, Michigan 48109*
Yevgeny Raitses†
*Princeton Plasma Physics Laboratory, Princeton, New Jersey 08543*
Noah Hershkowitz‡
*University of Wisconsin–Madison, Madison, Wisconsin 53706*
and
Michael McDonald§
*Naval Research Laboratory, Washington, D.C. 20375*

DOI: 10.2514/1.B35697

**This article provides recommended methods for building, operating, and taking plasma potential measurements from electron-emitting probes in electric propulsion devices, including Hall thrusters, gridded ion engines, and others. The two major techniques, the floating point technique and the inflection point technique, are described in detail as well as calibration and error-reduction methods. The major heating methods are described as well as the various considerations for emissive probe construction. Special considerations for electric propulsion plasmas are addressed, including high-energy densities, ion flows, magnetic fields, and potential fluctuations. Recommendations for probe design and operation are provided.**



## Nomenclature

| | | |
|---|---|---|
| $A_G$ | = | material-specific Richardson's constant, $A \cdot m^{-2} \cdot K^{-2}$ |
| $A_0$ | = | universal Richardson's constant, $A \cdot m^{-2} \cdot K^{-2}$ |
| $a$ | = | probe radius, m |
| $C$ | = | capacitance, F |
| $C_p$ | = | specific heat capacity, J/K |
| $E$ | = | Young's modulus, Pa |
| $f$ | = | frequency, Hz |
| $I$ | = | electric current, A |
| $k_B$ | = | Boltzmann's constant |
| $m$ | = | mass, kg |
| $N$ | = | number |
| $n$ | = | number density, $m^{-3}$ |
| $R$ | = | resistance, Ω |
| $R_0$ | = | resistance of plasma, Ω |
| $r_{L,e}$ | = | electron Larmor radius, m |
| $S$ | = | surface area, $m^2$ |
| $T$ | = | temperature, eV |
| $t$ | = | time, s |
| $V$ | = | electric potential, V |
| $v$ | = | velocity, m/s |
| $\alpha$ | = | floating potential correction factor |
| $\Gamma$ | = | flux, $m^{-2} \cdot s^{-1}$ |
| $\hat{\Gamma}$ | = | ratio of emitted to collected electron flux |
| $\delta$ | = | probe size parameter |
| $\epsilon$ | = | emissivity |
| $\lambda_d$ | = | debye length, m |
| $\lambda_{i-n}$ | = | ion-neutral mean free path, m |
| $\lambda_R$ | = | material-specific factor |
| $\rho$ | = | mass density, $kg/m^3$; or electrical resistivity, Ω m |
| $\sigma$ | = | Stefan–Boltzmann constant, $J \cdot s^{-1} \cdot m^{-2} \cdot K^{-4}$; or standard deviation |
| $\phi$ | = | space potential, V |
| $\phi_p$ | = | plasma potential, V |
| $\phi_W$ | = | work function, V |

*Subscripts*

| | | |
|---|---|---|
| amb | = | ambient |
| $B$ | = | Bohm |
| $b$ | = | probe bias |
| $c$ | = | critical |
| $c0$ | = | electron saturation current |
| $e$ | = | plasma electron |
| em | = | emitted electron |
| et | = | temperature-limited emission |
| $e0$ | = | temperature-limited emission current |
| $f$ | = | floating |
| $H$ | = | heating |
| $I$ | = | inflection point |
| $i$ | = | ion |
| max | = | maximum |
| min | = | minimum |
| $S$ | = | separation point between temperature- and space-charge-limited emission |
| $s$ | = | at the sheath edge |
| sheath | = | across the sheath |
| traces | = | I-V traces |
| vc | = | virtual cathode |
| $w$ | = | wall or wire |

*Superscripts*

| | | |
|---|---|---|
| cold | = | nonemitting or cold |
| em | = | emitting or hot |
| exp | = | experimentally determined |
| * | = | electron saturation |

Presented as Paper 2013-313 at the International Electric Propulsion Conference, Washington, D.C., 6–10 October 2013; received 16 December 2014; revision received 9 August 2016; accepted for publication 9 August 2016; published online 3 November 2016. 

*Assistant Research Scientist, Aerospace Engineering, 1320 Beal Avenue. Member AIAA.
†Principal Physicist. Member AIAA.
‡Emeritus Professor, Engineering Physics, 1500 Engineering Drive.
§Aerospace Engineer. Member AIAA.

## I. Introduction

ALONG with temperature and density, plasma potential is one of the most important parameters of a plasma. Langmuir [1] recognized the importance of the potential structure for the role it played in confining electrons in his first experiments. Today, the plasma potential is often measured because it is a principal factor in understanding a wide range of phenomena from confinement to charged particle flows [2–6]. For aerospace applications, measurements of the plasma potential enable the deduction of the electric field that accelerates ions and heats electrons in plasma thrusters and their plumes [7]. Although the potential can be measured with Langmuir probes in some plasmas, these techniques fail in many circumstances, such as in the presence of flowing plasma typical for aerospace applications, and are subject to large uncertainties, such as in the presence of magnetic fields [5,8–10]. Energy analyzers or laser-induced fluorescence can be used to determine ion velocities [11], which can be used to deduce the plasma potential. However, the use of these techniques is not so straightforward for complex, multidimensional flow, such as expanding plasmas. Among all existing direct and indirect measurement techniques of the plasma potential, emissive probes can be not only the most simple in practical implementation and interpretation, but also produce measurements with the least uncertainty [12–14].

The first concept of an electron-emitting probe was proposed by Langmuir [1] in 1923, at the same time as when he proposed the collecting probe, now called the Langmuir probe. Langmuir probes can be used to find the plasma potential by identifying the knee in the current–voltage (I-V) characteristic curve [8] or by the inflection point [15]. Emissive probes, however, can determine the plasma potential more precisely, down to $T_e/10e$ for a high-signal-to-noise ratio. Here $T_e$ is the electron temperature in electron volts of a Maxwellian plasma. If the plasma is not Maxwellian, $T_e$ should be interpreted as an effective electron temperature. A typical physical construction of the emissive probe is shown in Fig. 1 [14]. The 0.0025-cm diameter tungsten wire is exposed to the plasma and a current is passed through it to heat the wire so that it emits electrons.

To briefly explain the concept of an electrically floating emissive probe, recall that, for typical plasma conditions, a very thin layer, the so-called sheath, is always formed near a plasma-facing surface. In a low-temperature plasma, the surface is always charged negatively by electrons with respect to the plasma due to the much higher mobility of electrons as compared with heavier ions. Therefore, the electric field in the sheath region accelerates electrons away from the emitting surface and is responsible for a very large reduction of electron heat and particle fluxes from the plasma to the surface. Figure 2 shows sheath potentials and particle fluxes. A typical voltage potential

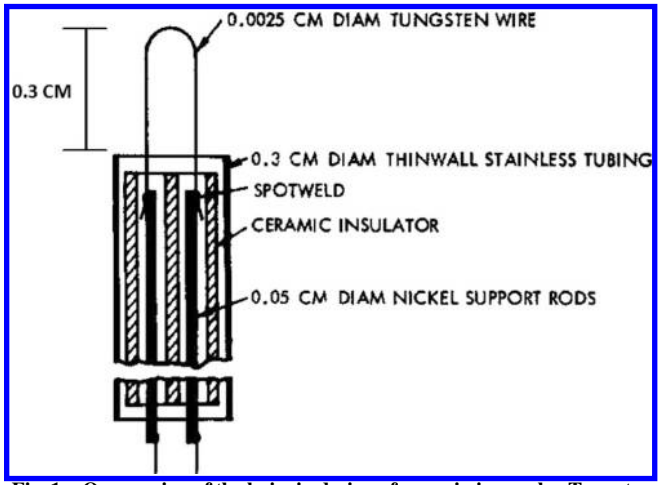


**Fig. 1 One version of the hairpin design of an emissive probe. Tungsten wire is the emissive probe filament and the rest of the structure connects the emissive probe electrically to the control circuit and mechanically secures the probe. (Reproduced from Kemp and Sellen [14], with permission from AIP Publishing.)**

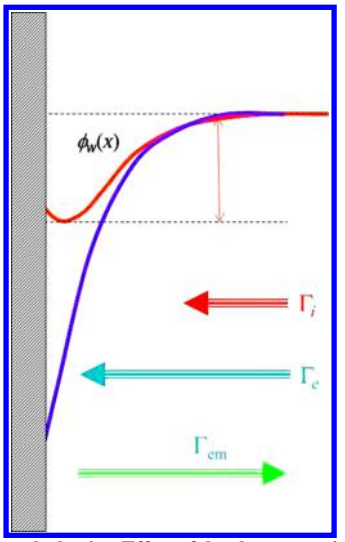


**Fig. 2 Emissive probe basics: Effect of the electron emission on the near-wall sheath (according to the fluid description of Hobbs and Wesson [2]). Plasma fluxes to the floating emitting surface, including electron flux $\Gamma_e$, ion flux $\Gamma_i$, and flux of emitted electrons from the surface $\Gamma_{em}$, are balanced to maintain zero net current to the floating surface. The voltage drop across the sheath $\phi_{sheath}$ reduces as the flux of emitted electrons approaches the flux of collected electrons from the plasma. The Langmuir sheath, with no emitted electrons, is the lower potential whereas the emissive sheath is the upper.**

difference between plasma and the surface ranges from a few to several $T_e/e$, depending mainly on the ion mass and the electron energy distribution function (EEDF). For example, for xenon gas and a Maxwellian EEDF, the potential difference is $5.75T_e/e$. When electrons are emitted from the surface, they can reduce negative charge on the surface. As a result, the voltage drop in the sheath between the plasma and the surface decreases with increased electron emission (Fig. 2). This idea of having an emitting surface float at the plasma potential is the basic principle of operation of the floating emissive probe technique. In most practical applications, the temperature of plasma electrons is much higher than the temperature of emitted electrons, which is on the order of the emitting surface temperature. Therefore, the floating potential of the emitting surface always remains below the plasma potential due to so-called space-charge effects associated with this temperature difference. For example, for a Maxwellian EEDF, the potential difference between the plasma and the surface is between 1 and 2 plasma electron temperatures, depending on collisionality and geometry.

The emissive probe can be electrically floating or biased with respect to some reference potential. The floating emissive probe is generally a less accurate method of the determination of the plasma potential than the biased probe, but its electrical circuitry and data analysis are much simpler. These advantages make the floating emissive probe attractive for the use on spacecraft [16,17]. Floating probes can also be useful in harsh plasma environments, for example, plasma thrusters where the probe should be introduced or operated for less than a second at a time. When an emitting probe is biased more negatively than the plasma potential, electrons can be emitted from the probe into the plasma because the electric field accelerates the electrons from the surface into the plasma. When the emitting probe is biased more positively than the plasma potential, electrons cannot be emitted, except for a small number with high energies in the tail of the emitted electron distribution.

Experimentally obtained emissive probe I-V traces are shown in Fig. 3 [12]. In these traces, the plasma potential is approximately −21 V. When the probe is biased below this potential, there is significant emitted current (which is read on the graph as negative probe current). Above the plasma potential, electrons are predominantly collected rather than emitted. The increasing wire temperature corresponds to increasing electron emission, resulting in the increasing magnitude of the current for the more negative probe

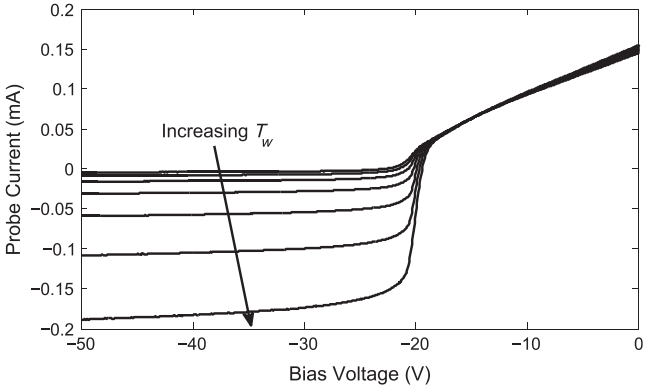


**Fig. 3 Experimental emissive probe I-V traces with current from the probe on the vertical axis and probe bias voltage on the horizontal axis. (Reproduced from Sheehan and Hershkowitz [12], with permission from IOP Publishing.)**



biases. This feature is an unambiguous indicator of the plasma potential. Although the inflection point of a Langmuir probe I-V trace indicates the plasma potential, emissive probe techniques can reduce uncertainty [10] and provide accurate measurements even with the added complications of particle beams or sheaths (see Secs. VI.C and VI.E).

This article seeks to provide a rigorous review of the practical implementation of emissive probes in electric propulsion devices. It draws from material presented in the general review of emissive probes [12], refining and expanding to best suit the needs of the electric propulsion community. In Sec. II, emissive probe and emissive sheath theory are presented, though it is meant to serve only as an introduction to this topic. The state-of-the-art methods for using emissive probes to measure the plasma potential are described in Sec. III, along with calibration and error-reduction techniques. The methods are also compared in this section. There are a variety of ways to heat a probe to emission and these are described in Sec. IV. Section V contains details on the specifics of building an emissive probe, including filament size and shape. There are a number of special cases in which emissive probes can be used that warrant special consideration (Sec. VI). Section VII contains discussion on how to choose the design and technique given a specific electric propulsion device followed by the conclusions in Sec. VIII.

## II. Emissive Probe Theory

This section describes the physical processes driving emissive probe operation and, in the case of swept emissive probes, the shape of their I-V traces. Emissive sheaths are analyzed using simple planar emitter models, the effects of space charge on those models, and finally the differences encountered with more realistic cylindrical emitter models.

### A. Simplified Models

#### 1. Floating Emissive Probe

Zero net current flows through the sheath of isolated bodies such as dielectric or electrically floating metal surfaces. Assuming a Maxwellian distribution for the electrons, the electron flux from the plasma is $\Gamma_e = (1/4)n_s v_e \exp(-e\phi_{\text{sheath}}/T_e)$, where $n_s$ is the electron density at the sheath edge, $\phi_{\text{sheath}}$ is the sheath potential (the potential difference between the sheath edge and the surface), $v_e = \sqrt{8T_e/\pi m_e}$ is the thermal velocity of the electrons, $T_e$ is the electron temperature in electron volts, and $m_e$ is the electron mass. The ion flux $\Gamma_i = n_s v_B$ is due to the nonzero ion velocity at the sheath edge as necessitated by Bohm's criterion: $v_B \geq \sqrt{T_e/m_i}$, where $m_i$ is the ion mass [18]. Bohm's criterion is assumed to be fulfilled marginally (i.e., in equality), which is typical in nonflowing plasmas. Equating these fluxes allows the potential of the sheath surrounding a planar floating surface to be calculated:

$$\phi_{\text{sheath}} = -\frac{T_e}{e}\ln\left(\sqrt{\frac{m_i}{2\pi m_e}}\right) \tag{1}$$

Because electrons are much more mobile than ions ($m_e \ll m_i$), the surface is always negative compared with the plasma potential in low-temperature plasmas. In this paper, space potentials in the plasma are denoted as $\phi$, whereas electric potentials of solids are notated as $V$, both with units of volts.

The floating potential of emitting surface facing the plasma is determined by the balance of electron and ion fluxes from the plasma and the flux of emitted electrons from the wall:

$$\Gamma_i + \Gamma_{\text{em}} - \Gamma_e = 0 \tag{2}$$

Hobbs and Wesson [2] used a fluid description of the sheath surrounding a planar electron-emitting surface to calculate the floating potential of that surface as a function of the ratio of emitted electron flux to collected electron flux $\hat{\Gamma}$:

$$\phi_{\text{sheath}} = -\frac{T_e}{e}\ln\left(\frac{1-\hat{\Gamma}}{\sqrt{2\pi m_e/m_i}}\right) \tag{3}$$

assuming that $T_e \gg T_i$. This equation indicates that, as the level of electron emission is increased, the sheath voltage drop will decrease (as indicated in Fig. 2). However, for a quasi-neutral plasma, $\hat{\Gamma}$ does not reach one due to space-charge effects described in Sec. II.B.

#### 2. Biased Emissive Probe

There are two basic components to the emissive I-V curve: the collected electron current and the emitted electron current. Ion current is neglected in this description because it is much less than the temperature-limited emission current. For example, in a xenon plasma, the electron saturation current is nearly 500 times larger than the ion saturation current. The temperature-limited emission current for biased emissive probes is typically 10% of the electron saturation current, making it over an order of magnitude larger than the ion saturation current. Even in the presence of a thruster ion beam with an energy $2000T_e$, the emitted current will dominate the ion current. When the ion current is on the order of the electron current, then its effects must be taken into account, but that is not a common case for electric propulsion plasmas.

It is useful to examine the equations describing the electron currents in the simple case of a cylindrical probe with space-charge effects neglected. These simple equations can yield a qualitative understanding of how emissive probes work. Space-charge effects are caused by nonneutral charge buildup around the probe and significantly complicate calculations (see Sec. II.B).

The collected electron current $I_e$ is the same as that of a cold Langmuir probe [8,19,20]:

$$I_e(V_b) = \begin{cases} I_e^* \exp\left(\frac{-e(\phi_p - V_b)}{T_e}\right), & V_b \leq \phi_p \\ I_e^* g_e(V_b - \phi_p), & V_b > \phi_p \end{cases} \tag{4}$$

where $V_b$ is the probe bias, $\phi_p$ is the plasma potential, $I_e^*$ is the electron saturation current, and the function $g_e(V_b - \phi_p)$ accounts for angular momentum of the collected electrons. The emitted current can be written as

$$I_{\text{em}}(V_b) = \begin{cases} I_{\text{et}}, & V_b < \phi_p \\ I_{\text{et}} \exp\left(\frac{-e(V_b - \phi_p)}{T_{\text{em}}}\right) g_{\text{em}}(V_b - \phi_p), & V_b \geq \phi_p \end{cases} \tag{5}$$

The function $g_{\text{em}}(V_b - \phi_p)$ accounts for the angular momentum and probe radius effects on the emitted electrons and $T_{\text{em}}$ is the emitted electron temperature in electron volts [8]. Temperature-limited emission $I_{\text{et}}$ for thermionic emission is given by the Richardson–Dushman equation, which is [21]

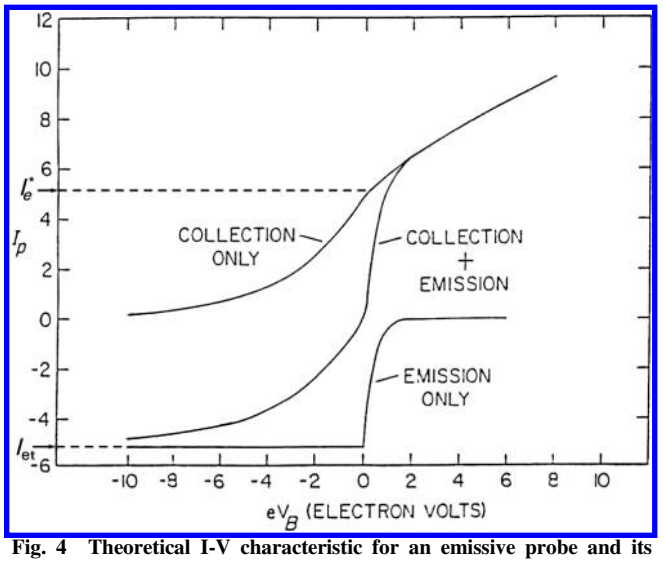


**Fig. 4 Theoretical I-V characteristic for an emissive probe and its collecting and emitting components. (Reproduced from Hershkowitz [8], with permission from Elsevier.)**

$$I_{\text{et}} = A_G T_w^2 S \exp\left(\frac{-e\phi_W}{T_w}\right) \tag{6}$$

$$A_G \equiv \lambda_R A_0 = \lambda_R \frac{4\pi m_e k_B^2 e}{h^3} \tag{7}$$

where $A_G$ is the material-specific Richardson–Dushman constant, defined as the product of a material-specific factor $\lambda_R \in (0, 1)$ and $A_0 = 120\ \text{A}/(\text{cm}^2 \cdot \text{K}^2)$, the universal Richardson–Dushman constant; $\phi_W$ is the work function of the wire; $S$ is the surface area of the wire; $k_B$ is Boltzmann's constant; and $h$ is Planck's constant [22]. Depending on the source, either $A_G$ or $\lambda_R$ may be found in the literature. For pure tungsten, $A_{G,W} = 60.2\,\text{A}/(\text{cm}^2 \cdot \text{K}^2)$ and for thoriated tungsten $A_{G,W/\text{ThO}} = 3\,\text{A}/(\text{cm}^2 \cdot \text{K}^2)$ [23].

Equations (4) and (5) are graphed in Fig. 4 with $V_p = 0$ and $T_e = 1$ eV [8]. Note that electron current is even emitted slightly above the plasma potential, between 0 and 1 V, due to electrons in the high-energy tail of the emitted EEDF able to overcome a probe bias equal to a few $T_w/e \approx 0.2$ V. At biases less than the plasma potential, the emission current is constant. In this regime, the wire's temperature limits the emission of electrons, so it is known as the temperature-limited regime. Figure 3 shows all of the same features as the theoretical graphs in Fig. 4.

### B. Space-Charge Effects

Although the aforementioned model is useful for gaining a basic understanding of how emissive probes work, it ignores an important aspect of emissive probes: space-charge effects. The additional flux of emitted electrons from the probe can significantly change the charge density in the sheath [2,24]. This effect was first noted in the context of a floating emissive surface and is critical to consider when using the floating point method for emissive probes (see Sec. III.A) [2]. The space-charge effects result from the fact that fluxes and temperatures of the plasma electrons collected by the emitting probe and the emitted electrons from the probe to the plasma are not equal.

Equation (3) is valid until the emission reaches a critical level $\hat{\Gamma}_c$ at which the electric field at the surface is zero [2]. This critical value is $\hat{\Gamma}_c \lesssim 1$ and depends on the ion-to-electron mass ratio. The sheath potential drop in space-charge-limited emission depends only on the electron temperature [2,25]:

$$\phi_{\text{sheath}} \approx -\frac{T_e}{e} \tag{8}$$

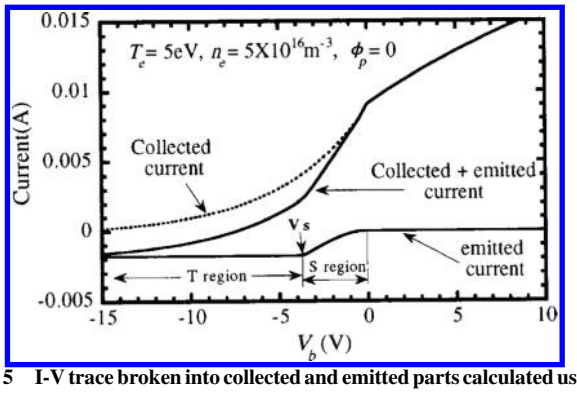


**Fig. 5 I-V trace broken into collected and emitted parts calculated using Ye and Takamura's model [28]. (Reproduced with permission from AIP Publishing.)**

If the surface is further heated in an attempt to increase the emission level, a virtual cathode will form around the surface, preventing additional electrons from escaping into the plasma (see the schematic depiction in Fig. 2) [24,26,27]. Once the virtual cathode has formed, some of the emitted electrons will escape into the plasma and some will be confined to the wall. This result is not predicted by the simple theory described in Sec. II.A, but is an important effect that cannot be neglected. The sheath potential drop will shrink slightly because the $\phi_{\text{vc}}$ (the potential at the virtual cathode minimum) stays constant while $V_w - \phi_{\text{vc}}$ increases, but that is typically insignificant unless $T_e \sim T_{\text{em}}$.

Space-charge effects alter the floating potential and the shape of the I-V trace near the plasma potential and below. The first analytical description of an emissive probe I-V trace considering space-charge effects was given by Ye and Takamura [28]. The equations necessary to fully describe the I-V trace are not reproduced here; the full derivation can be found in Ref. [26]. The model assumes cold ions, Maxwellian plasma electrons, emitted electrons at zero energy, a cylindrical collector, a planar emitter, and no secondary electrons [10]. A weakness of this model is the planar emitter, which should be cylindrical for emissive probes. Results obtained from these model equations are graphed in Fig. 5 [28]. The I-V trace is divided into three regions. In the region with probe biases $V_b$ above $\phi_p$, the current is strictly due to collected electrons. The region with probe biases below $V_S$ is the temperature-limited emission region (T region). These two are separated by the space-charge-limited region (S region) where the electron emission is dictated by the space-charge surrounding the probe rather than the temperature of the probe. It is bounded by $V_S$, the potential value that separates the T and S regions, and approximately $V_p$. This model accurately predicts that the floating potential will never get closer to the plasma potential than $\sim -T_e/e$. Preliminary experiments show good qualitative agreement to Ye and Takamura's model in [10,29].

### C. Cylindrical Model

All of the preceding theories are for planar emitters. Although planar emissive sheaths do exist, typically caused by secondary electron emission from the surface of vacuum vessels, emissive probes are almost always cylindrical (though occasionally spherical [30]). It is therefore important to understand how the geometry of the probe affects the sheath that forms around it. Emissive sheath theories in cylindrical geometries have only started to be developed in the last few years.

Fruchtman et al. [31] solved Poisson's equation in cylindrical coordinates assuming a Maxwellian EEDF, cold ions, and electrons emitted with zero energy. For large probe radii (much greater than the Debye length), they were able to find a two-scale solution. They solved Poisson's equation in the nonneutral sheath and the plasma equation (Poisson's equation with zero electric field) in the quasi-neutral presheath. This solution matched the planar solution given by Hobbs and Wesson [2]. For arbitrary probe radii $a$, they solved Poisson's equation numerically, matching the solution far from the probe to the plasma equation (see Fig. 6). When the probe radius is

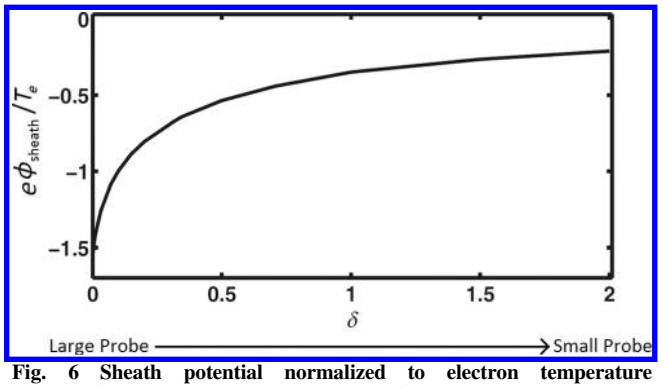


**Fig. 6 Sheath potential normalized to electron temperature ($e\phi_{\text{sheath}}/T_e$) vs inverse probe size ($\delta = \lambda_d/a$).**

small ($\delta = \lambda_d/a$ is large), the sheath potential is smaller, meaning that the probe floats closer to the plasma potential. As ions converge on the cylindrical probe, their density increases because the flux is constant through the sheath. With a cylindrical surface, the ion density is greater at the surface, which further reduces the sheath potential.

Initial investigations have begun into orbital motion effects on emissive sheaths. Orbital motion-limited (OML) probe theory uses single particle trajectories to determine particle currents as a function of bias potential on the probe [32]. For cylindrical and spherical probes, the electric field of the sheath surrounding the surface can attract charged particles that would have otherwise missed the probe, increasing the flux of these particles. For example, for a floating probe with an electron-repelling sheath, this OML situation could lead to the increase in the flux of ions collected by the probe. In addition, because high-energy electrons entering the OML sheath could miss the probe, the flux of electrons collected by the probe surface should also decrease. Because of these OML effects on ions and electrons, the floating potential of the probe in the OML regime should be higher than the floating potential of the probe when only radial motion is considered.

In addition to OML effects on collected charged particles, OML motion can alter the dynamics of electrons emitted from the probe. Robertson [33] considered the orbital effects of electrons emitted from a wire in a vacuum. Electrons are emitted from the surface with a two-dimensional Maxwellian distribution, so there is a velocity component in the azimuthal direction. By considering this aspect of electron emission, Robertson showed that the space-charge buildup in the sheath is larger than that predicted by the one-dimensional cylindrical model. Increased space-charge increases the curvature of the sheath and results in a larger sheath potential. To understand exactly how orbital motion affects an emissive probe, this theory must be extended to emissive sheaths in a plasma, but these initial results suggest that orbital motion may offset some of the sheath reduction caused by ion convergence.

## III. Methods for Determining the Plasma Potential

The principle use of an emissive probe is to determine the plasma potential using the fact that the probes will emit below the plasma potential, but not above it. There are a number of techniques that can be used to exploit this characteristic behavior [10,12].

### A. Floating Point with Large Emission

Over the years, the floating emissive probe technique has been used for a number of space applications, including satellite space potential [16], plasma potential measurements in plasma thrusters [7,34,35], etc. Furthermore, by measuring floating potential of a hot emissive and a cold nonemitting probe, it is possible to deduce the electron temperature [3,36,37].

#### *1. Operation: Measuring the Floating Potential*

The first major application of emissive probes was by Kemp and Sellen [14] in 1966. The floating potential of a probe is the

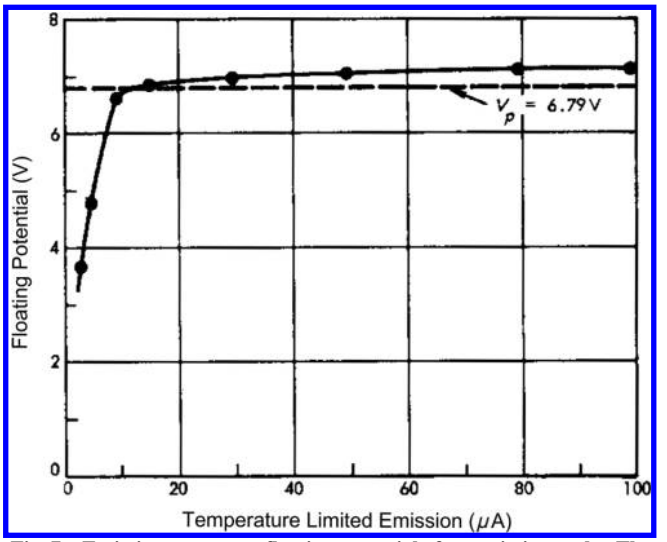


**Fig. 7 Emission current vs floating potential of an emissive probe. The dashed line indicates the measured plasma potential of 6.79 V. (Reproduced from Kemp and Sellen [14], with permission from AIP Publishing.)**

intersection of the I-V curve with the load line, the current–voltage curve of the electronics used to measure the current. The load line is the I-V curve in absence of the plasma that, in practice, has a linear relationship indicative of a resistor, occasionally with a constant offset caused by the electronics. For an ideal measurement, the load line is horizontal (no current is drawn regardless of the voltage) and the floating potential is where the current is zero. As the emission of the probe is increased from no emission, the floating potential of the probe rises rapidly at first, but plateaus near the plasma potential (see Fig. 7) [14]. After this point, increasing the emission only slightly changes the floating potential due to space-charge effects [24].

Generally, when using this technique, the emission is increased until the floating potential saturates. The technique is known as the floating potential in the limit of large emission, and many assume the value of the floating potential at saturation to be the plasma potential [14,37–39]. Kemp and Sellen [14] argued that the floating point method is viable for electron densities between $10^5$ and $10^{12}$ cm$^{-3}$. Below the lower limit, the electron saturation current is so small that space-charge effects dominate. Space-charge effects can change the plasma potential when the current emitted from the probe locally depresses the plasma potential, reducing the electron emission into the plasma. Above the upper limit, the filament temperature needed to reach high enough emission would melt the filament. Kemp and Sellen [14] claimed that, within this stated range, the plasma potential can be measured to within an accuracy of 0.01 V, but from emissive probe theory, the uncertainty cannot be better than $T_w/e$, typically 0.2 V [8].

Three factors complicate measuring the emissive probe floating potential: measuring from a remote location outside the vacuum chamber or satellite, measuring it while the probe is floating at tens or perhaps hundreds of volts above ground, and in time-resolved investigations, measuring the potential at sufficiently high frequency to capture phenomena of interest [39,40].

The floating potential of interest in an emissive probe is at the filament tip, whereas measurements are usually made outside the vacuum chamber. In the case of a dc heating current, filament resistance introduces a several-volt drop across the probe while the current is on. A four-wire sense configuration can remove errors due to line resistance, but because the majority of the drop is over the filament itself, the benefit is limited. If great accuracy is not required, the simplest option is to measure on one side or the other of the filament at the feedthrough and accept the error. Rectified ac heating with measurement during periods of zero current is also possible [41,42], but it complicates the circuit

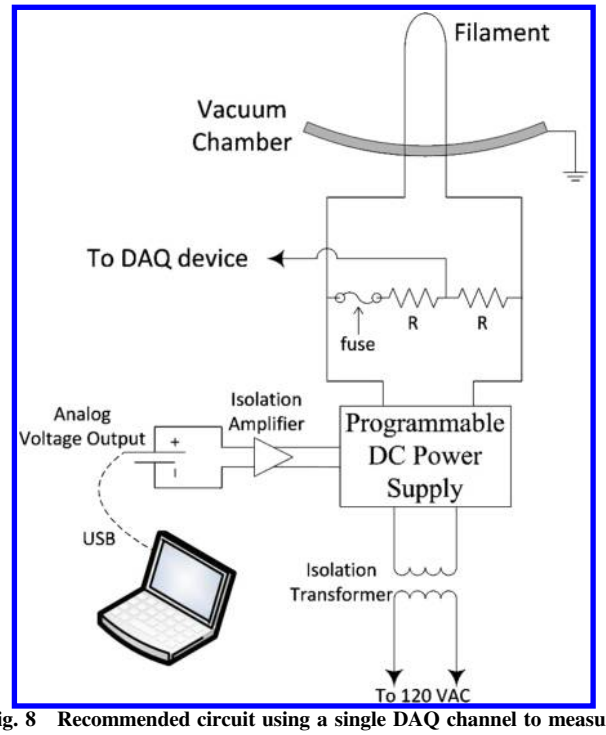


**Fig. 8 Recommended circuit using a single DAQ channel to measure probe potential. A compensated oscilloscope probe (not shown) is used to divide the large floating potential safely into the DAQ device. (Reproduced from McDonald et al. [43].)**

(see Sec. IV.B). Measuring the potential on each side of the filament at the feedthrough and averaging in postprocessing improves the accuracy. A preferred method requiring only one data acquisition channel is shown in Fig. 8 [43]. The measurement point is a tap between two matched series resistors placed in parallel with the filament resistance. These resistors should be large relative to the filament and line resistance such that minimal current flows through them during probe operation. A sacrificial fast-blow fuse protects the resistors in case of a current surge when a filament fails and the power supply attempts to force the commanded current across the resistors. Ideally, if the lead lines and resistors are perfectly matched and the fuse resistance is negligible, the filament tip voltage is identical to the resistor tap voltage. Practically, the tap potential should be calibrated to the filament potential by measuring both values simultaneously at atmosphere while sourcing small test currents of a few hundred milliamperes through the circuit.

The simplest method for determining the floating potential is to connect the emitting probe to ground through a resistor or a high-impedance isolation amplifier, such as an AD-210. Larger resistors have a more horizontal load line and more accurately measure the potential at which no current is drawn, so high resistances (in the M Ω range) are used when bandwidth is not an issue. Alternatively, the floating point can be measured by taking an I-V trace and finding the potential at which there is zero current. This method is much less convenient but is not affected by resistances. When the plasma density is very low, taking the I-V trace may be necessary to get an accurate reading of the plasma potential.

High floating potentials often prevent direct measurement by a data acquisition (DAQ) system or oscilloscope and require voltage division, isolation amplifiers, or both. Even for low plasma potentials, arcing or other unexpected events still pose a threat to a DAQ or scope. Several investigators have used large voltage dividers with MΩ-level resistors for DAQ protection but circuit protection by large resistance sacrifices measurement bandwidth. The resistive divider together with the stray capacitance in the lines and the power supply combine to form a low-pass resistor-capacitor (RC) filter with cutoff frequency

$$f_c = \frac{1}{2\pi RC} \tag{9}$$

where $R$ and $C$ are the line resistance and capacitance, respectively. Even a very low capacitance on the order of 10 pF (typical stray capacitance in coaxial cable is ∼100 pF/m) coupled with a 10 MΩ resistance will create a cutoff frequency at about 1 kHz. In practice, the probe frequency response is not quite as poor as the simple RC model would suggest, but numerous electric propulsion applications involve a signal on the order of tens of kilohertz or higher (e.g., the Hall thruster breathing mode). Moreover, power supplies may have millifarads of internal capacitance.

Instead, a combination of a low resistance $R$, a low-capacitance power supply, and a compensated oscilloscope probe enable wide bandwidth measurements with voltage division to acceptable levels for DAQ systems or oscilloscopes. Sizing the resistance $R$ to be about 50 times the hot filament resistance (which is a few ohms) ensures that only about 1% of the heating current passes through the resistors while avoiding low-pass filter effects. Some power supplies can bypass internal capacitors to reduce overall circuit capacitance significantly. Finally, compensated oscilloscope probes, also known as passive or attenuation probes, combine a resistive and capacitive voltage divider with a tunable capacitance such that, by matching the tunable capacitance on the probe to that of the DAQ or oscilloscope, they can provide constant voltage division regardless of frequency up to the probe bandwidth. Bandwidths up to gigahertz are available, though most fall in the megahertz range. Minimizing $R$ and the circuit capacitance makes sure the signal is not low-pass filtered before it even reaches the compensated probe, whereas properly tuning the probe preserves the signal bandwidth while dividing it to pass into the DAQ or scope. Tuning is accomplished by adjusting the probe capacitance until it can accurately reproduce the sharp corners and flat top of a moderate frequency (∼ kilohertz) square wave. With a properly chosen low-capacitance power supply and good probe tuning, this technique can achieve 1 MHz frequency resolution.

The most common devices for data acquisition are an oscilloscope or a DAQ device or card. Oscilloscopes provide higher bandwidth than DAQ systems, often gigahertz level instead of kilo- to megahertz, at the cost of fewer digital bits of resolution, usually 8 or at most 12 bits for an oscilloscope, compared with 16 bit for most DAQ systems. Oscilloscopes also typically accept larger input voltage ranges than DAQ systems. However, DAQ devices are often simpler to integrate into automated experiments, for example, using LabView software, and can continuously acquire data at peak frequency, whereas scopes have limited memory buffers. Even when planning to use a DAQ system for measurements, an oscilloscope is a simpler and safer device with which to start for checking voltage ranges, noise levels, and other initial troubleshooting.

An advantage of digital oscilloscopes for measurements is their increasingly common "high-resolution" capability to sacrifice bandwidth for digital resolution and noise reduction. For example, consider an oscilloscope with 4 GHz bandwidth, 8 bit resolution, and a memory buffer of $10^6$ points per channel. In normal operation, the scope fills the buffer completely, so that a 1 s acquisition would be at 1 MHz, 500 ms at 2 MHz, and so on. In this mode, the scope samples at 4 GHz, but for the 1 s acquisition, only one point each microsecond is recorded and the rest are thrown out. In high-resolution acquisition mode, each recorded point is generated by averaging all points acquired in the corresponding window. This reduces the measurement error by a factor of $N^{1/2}$, where $N$ is the number of averaged samples. At the example 4 GHz bandwidth for a 1 s, 1 MHz acquisition, an average of 4000 measurements produce each recorded value. In terms of digital bits, this increases the resolution by $\log_4(4\text{ GHz}/4\text{ MHz}) = 5$ bits to 13 bit resolution, or about 10 mV on a 100 V full scale. Of course, this increase in digital resolution comes at the cost of effectively low-pass filtering the signal.

### 2. *Calibration: Choosing a Heating Current*

Choosing the correct heating current for a floating emissive probe is a trial and error process. The heating current must bring the filament to sufficiently strong emission to form a virtual cathode and

saturate the floating potential. Too much heating, however, and the probe will burn out or suffer a significantly reduced lifetime. In practice, this current will vary slightly due to construction variation, even among similarly built probes, and can vary widely across probes of different designs. This section first describes the basic technique for finding the correct heating current in a given application, then gives a more general description of probe heating physics to approximate heating currents for a given probe size, sufficient to allow power supply sizing and circuit design.

To determine the optimum heating current for the floating emissive probe, the floating potential should be measured as the probe heating is increased. Initially, the floating potential will be almost independent of the probe heating current because negligible emission current is released at low temperature. Eventually, as the probe is heated, the floating potential will increase rapidly. Above a certain current, the rate of increase in floating potential of the now-hot probe with heater current will drop to a much lower value, as shown in Fig. 7. The amount of heating that causes the floating potential of the emissive probe to be just barely saturated is ideal for use in the floating point technique. The critical emission current, however, depends on the plasma in which the probe is situated; larger plasma densities require larger emission currents to saturate the floating potential. Be sure, then, that the amount of probe heating is sufficient to saturate the floating potential at all conditions where the plasma potential will be measured. This consideration can be particularly important, for example, when interrogating the discharge channel of Hall thrusters where the dense internal plasma requires much higher emission currents than the more tenuous far-field plasma. Even slightly underestimating the amount of heating needed to saturate the floating potential can lead to significant errors in measuring the plasma potential [14].

The temperature of a filament for a given heating current depends on a power balance between ohmic $I^2R$ heating and cooling by several mechanisms: conductive cooling to the filament ends, Stefan–Boltzmann radiative cooling, and cooling due to energy carried away by the thermionically emitted electrons. In the limit of a long wire ($l \gg a$), where conductive losses can be neglected, and treating the filament as a gray body with emissivity $\epsilon$, this power balance for a length of filament is

$$I^2R = \epsilon\sigma S(T^4 - T_{\text{amb}}^4) + \phi_W I_{\text{em}} \tag{10}$$

with ohmic heating on the left-hand side and radiative and thermionic cooling on the right-hand side, where $S$ is the radiative surface area $2\pi al$ of a segment of wire and $\sigma$ is the Stefan–Boltzmann constant. Because the work function is typically an order of magnitude larger than the emitted electron temperature, the additional energy loss coming from the tail of the emitted electron energy distribution is negligible. Expanding the terms in Eq. (10) and solving for the current $I$ yields

$$I = \left\{\frac{2\pi a^3}{\rho}\left[\sigma\epsilon(T_w^4 - T_{\text{amb}}^4) + \phi_W A_G T^2 \exp\left(\frac{-e\phi_W}{k_B T}\right)\right]\right\}^{1/2} \tag{11}$$

This complicated equation is made more so because the electrical resistivity $\rho$ is itself a strong function of temperature and the emissivity $\epsilon$ varies with both wavelength and filament surface condition. Nevertheless, it is clear that, for a given temperature in the long-wire limit, the heating current goes $I \propto a^{3/2}$. Figure 9 presents filament temperatures versus heating current for three filament diameters ($d = 2a$) using a gray body emissivity $\epsilon = 0.4$, $\phi_W = 2.6$ eV and $A_G = 3$ A/(cm$^2 \cdot$ K$^2$) for thoriated tungsten, and including $\rho = \rho(T)$ effects.

For example, Haas and Gallimore [37] reported heating currents in the range of 4.5–6.0 A using a 0.125-mm diameter filament for internal Hall thruster discharge channel measurements. The Hall thruster channel has a typical peak plasma density of order $10^{13}$ cm$^{-3}$ and electron temperature of 30 eV, for a thin-sheath cylindrical electron saturation current density of about $1.5 \times 10^5$ mA/cm$^2$. This value corresponds to the thermionic emission current density for

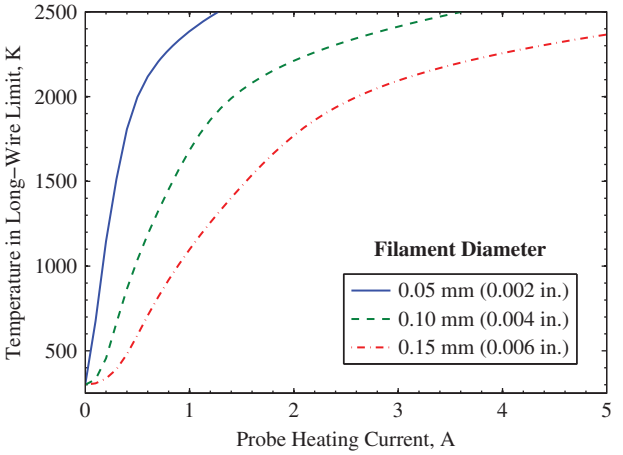


**Fig. 9 Emissive probe temperature under varied heating currents and filament diameters, using a simple application of the long-wire limit of Eq. (11). These curves should be treated as only approximate for real probes because they do not account for conductive cooling.**

thoriated tungsten at about 2500 K using the Richardson–Dushman equation. This range of heating currents and temperature lies in the upper right corner of Fig. 9 for Haas and Gallimore's filament [37], which has an intermediate diameter between the 0.10- and 0.15-mm diameter filaments shown.

Equation (11) and Fig. 9 are intended to be illustrative, not prescriptive. It must be emphasized that the proper heating current for a given application requires the careful search for saturation of the floating potential with increasing heating current as noted earlier. The main differences between the preceding simple model and a real filament are losses due to conductive cooling through the probe lead wires and body and any additional heating encountered by the probe in a dense plasma. To illustrate the importance of conduction, a filament with ends clamped at room temperature would require $l/a$ larger than about 200 for the filament tip temperature to match the long-wire limit. Real probes will have hot lead wires well above room temperature, relaxing $l/a$, but it is still likely that Fig. 9 will underestimate the required heating current for a given temperature in most real probes.

### 3. *Data Reduction and Error Analysis*

The floating potential of a highly emitting probe is less than the plasma potential by between $1.5T_e/e$ and $2T_e/e$, depending on the details of the EEDF and presheath. Errors in measuring the plasma potential using this method come from the measurement of the floating potential, the numerical factor $\alpha$ applied to $T_e$ such that $V_f = \phi_p - \alpha T_e$, and the estimation of $T_e$ itself, which must be determined separately. Hobbs and Wesson [2] considered a floating emitting surface in a plasma and solved Poisson's equation with Bohm's criterion modified for an emitting surface and determined that the potential of the floating surface was approximately $T_e$ below the potential at the sheath edge in the limit of large emission (see Sec. II.B) [2]. Numerical simulations show that a floating probe in the limit of large emission (emission current greater than collection current) will float $1.5T_e$ below the plasma potential [44]. In plasmas with a significant density of energetic electrons, such as in beam plasmas or double plasma devices [45], the floating point in the limit of large emission can approach the stopping voltage of the energetic electron energy and fail to provide an accurate plasma potential measurement [9,46]. If the EEDF is spatially constant for all measurements, then the differences between the plasma potential measurements (which are often of greatest interest, i.e. for electric field measurements) would be unaffected. To determine if the floating potential measurement is seriously affected by this offset, the floating potential technique can be compared with the inflection point technique (see following section).

Aside from any errors, the floating potential signal may be noisy; we recommend reporting one-half of the peak-to-peak fluctuations in

the floating potential as uncertainty. Typically these fluctuations come from the plasma, and so quiet, stable plasmas will have lower uncertainty for this technique. Heating source stability also reduces error, because small changes in probe temperature can greatly affect the emission current [see Eq. (7)]. Finally, long wires separating the probe and the measurement location can introduce electrical interference; keeping wires as short as possible and using coaxial cables when practical will reduce interference.

There is no simple analytical expression for the floating potential of an emissive probe, even in the planar model. Hobbs and Wesson [2] considered a floating emitting surface in a plasma, solved Poisson's equation with Bohm's criterion modified for an emitting surface, and determined that the potential of the floating surface was approximately $T_e$ below the potential at the sheath edge in the limit of large emission. However, there is an additional drop of $0.5–1T_e$ from the presheath, depending on collisionality. This factor can neither be neglected, nor easily measured. It was shown that, in the case $a \gg \lambda_d$, the floating potential saturates at [24,36]

$$V_{\mathrm{f}}^{\mathrm{em}} \approx \phi_p - 1.5T_e + \Delta\phi_{\mathrm{vc}} \tag{12}$$

where $\Delta\phi_{\mathrm{vc}}$ is the potential difference between the floating potential and the potential minimum (or virtual cathode; see Fig. 2) due to space-charge effects. For typical plasma thruster conditions $T_e \gg T_w$, the last term on the right-hand side is small, $\Delta\phi_{\mathrm{vc}} < 0.15T_e$. Recent plasma thruster experiments with floating emissive probes concluded that the full difference between the floating point in large emission and plasma potential was $1.5–2T_e$, consistent with the preceding values.

Note that for the determination of the plasma potential from Eq. (12) it is necessary to measure the electron temperature. When sweeping probes that are biased with respect to the plasma are not practical, the electron temperature can be measured by using double probes [47,48], triple probes, or even the same emissive probe when it is cold (nonemitting) or hot (strongly emitting). The method of determining the electron temperature $T_e$ from the floating potentials of the cold and hot cylindrical emissive probe relies on knowledge of the electron and ion currents drawn by the probe at a given potential [24,36]. In general, the floating potential of a probe adjusts itself so that the probe draws no net current in a steady state. Thus, the floating probe retards the incident electrons and attracts the ions. In the case of the retarding potential, the electron current to the cylindrical probe is well known and given by [49]

$$I_e(V_b) = \frac{en_eS}{4}\sqrt{\frac{8T_e}{\pi m_e}}\exp\left(\frac{e(V_b-\phi_p)}{T_e}\right) \tag{13}$$

This current is independent of the sheath size, which is not the case for the ion current to the attracting probe. In general, the current of charge carriers to the attracting probe depends on the ratio $a/\lambda_d$ [49,50].

For a probe radius large with respect to the debye length ($a \gg \lambda_d$), the probe is in the well-known thin (planar) sheath limit, which requires that ions be accelerated to the Bohm velocity before entering the sheath [18]. In this case, all ions entering the sheath are collected by the probe and, equating the ion and electron fluxes, the floating potential of a cold probe in the thin-sheath limit is

$$V_{\mathrm{fl}}^{\mathrm{cold}} = \phi_p + T_e \ln\left(0.61\sqrt{\frac{2\pi m_e}{m_i}}\right) \approx \phi_p - 5.77T_e \tag{14}$$

where $m_i$ is the mass of a xenon atom in this case. Recall that $V_{\mathrm{fl}} - \phi_p$ is the potential difference between the bulk plasma potential and the surface, whereas $\phi_{\mathrm{sheath}}$ is the potential difference between the sheath edge and the surface, the difference between the two being the presheath potential. The factor of 0.61 comes from the density drop between the bulk plasma and the sheath edge due to the presheath in a collisionless plasma. In the opposite limiting case of a thick sheath ($a \ll \lambda_d$), the simple analytical expressions exist if the potential around the probe decreases more slowly than $r^{-2}$. Under these assumptions, the probe is in the OML regime [19]. In this regime, for every ion energy there exists an impact parameter that makes the ion hit the probe with a grazing incidence. The maximum impact parameter for hitting the probe is then a simple function of the ion initial energy and the probe potential. The ion current to the probe is given in this case by

$$I_i(V_b) = \frac{2en_iS}{\sqrt{\pi}}\sqrt{\frac{-e(V_b-\phi_p)}{2\pi m_i}} \tag{15}$$

It is important to emphasize that the OML current is the maximum ion current that can be collected by a cylindrical probe with a given collection area. Then, by equating the electron and ion currents [Eqs. (13) and (15)], the floating probe potential satisfies the equation

$$\frac{4m_e}{\pi m_i} = \frac{T_e}{e(\phi_p - V_{\mathrm{fl}}^{\mathrm{cold}})}\exp\left(\frac{2e(V_{\mathrm{fl}}^{\mathrm{cold}}-\phi_p)}{T_e}\right) \tag{16}$$

The numerical solution of this equation for xenon plasma gives the floating potential in the thick-sheath limit of the OML regime:

$$V_{\mathrm{fl}}^{\mathrm{cold}} = \phi_p - 5.24T_e \tag{17}$$

Thus, the absolute value of the floating potential in the thick-sheath case is about 10% smaller than that in the thin-sheath case. The floating potential shifts closer to the plasma potential.

As the ratio $a/\lambda_d$ increases and becomes $a/\lambda_d \sim 1$, the OML theory breaks down. This happens because of the specific potential distribution around the probe in this case, which can reflect ions that would not be reflected in the simpler (e.g., Coulomb-like) potential. The case of arbitrary ratio $a/\lambda_d$ is very complex and can be treated only numerically. The corresponding problem was formulated and studied by Bernstein and Rabinowitz [51] and Laframboise [52]. The numerical results in [52] were later fitted with rather simple analytical expressions by Steinbrüchel [53]. According to Steinbrüchel, the OML current [Eq. (15)] remains a very good approximation to the numerical results for $a/\lambda_d < 3$. However, for arbitrary $a/\lambda_d$ the value of the floating potential of a cold probe lies between the upper and the lower bounds given by Eqs. (17) and (14), respectively.

For example, for the typical Hall thruster discharge channel plasma parameters $n_e \sim 5 \times 10^{11}$ cm$^{-3}$ and $T_e \sim 20$ eV, the Debye length is about $\lambda_d \sim 0.05$ mm. The hotter or less dense the plasma is, the larger the debye length is. If the emissive probe diameter is ~0.1 mm, $a/\lambda_d \sim 1$, and the planar probe approximation does not apply. In fact, according to Steinbrüchel [53], the OML theory is more appropriate to calculate the ion current and the floating potential. In the following, the maximum uncertainty that is introduced in the value of $T_e$ is estimated when one uses the planar probe model to determine $T_e$ from the measured floating potentials of the cold and hot cylindrical emissive probe. In the planar probe model, the electron temperature can be found from Eqs. (12) and (14):

$$T_e^{\mathrm{exp}} = \frac{V_f^{\mathrm{em}} - V_f^{\mathrm{cold}}}{4.27} \tag{18}$$

this experimentally measured temperature $T_e^{\mathrm{exp}}$ should be distinguished from the true value of the electron temperature $T_e$. The real $T_e$ should be determined from the appropriate formulas for the cylindrical probe. For the cold probe in the case $a \sim \lambda_d$, we can use Eq. (17), whereas for the hot emissive probe, the equation is

$$V_f^{\mathrm{em}} \approx \phi_p - \alpha T_e \tag{19}$$

Here the coefficient $\alpha$ is larger than zero, because the floating potential of the emissive probe should be less than the plasma potential. On the other hand, as follows from the comparison with the thin-sheath case, $\alpha < 1.5$. Thus,

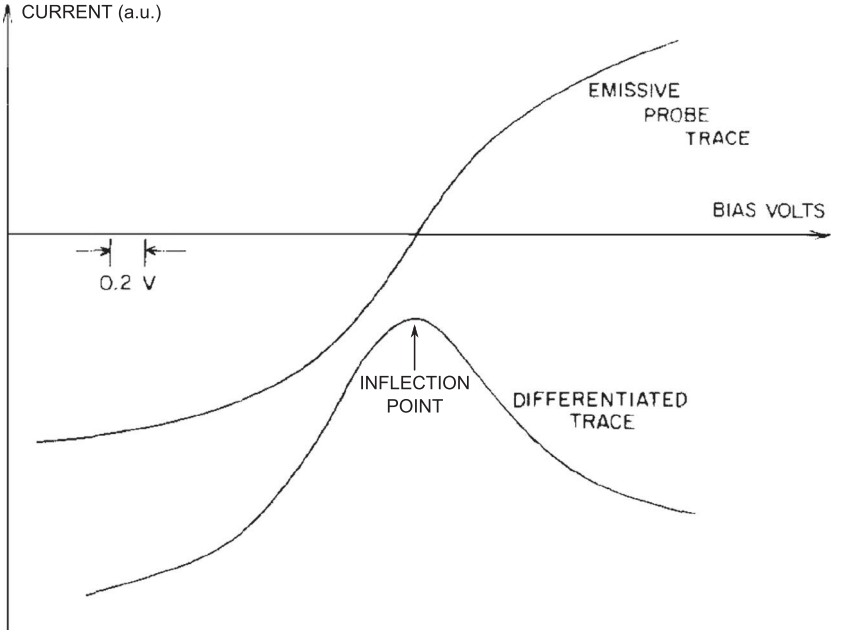


**Fig. 10 An experimental emissive probe I-V trace (with the current in arbitrary units (a.u.)) and its derivative, which is used to determine the inflection point. (Reproduced from Smith et al. [20], with permission from AIP Publishing.)**

$$T_e = \frac{V_f^{\text{em}} - V_f^{\text{cold}}}{5.24 - \alpha} = \frac{4.27 T_e^{\text{exp}}}{5.24 - \alpha} \tag{20}$$

The maximum possible value of $T_e$ is $T_e(\alpha = 0) = 0.815 T_e^{\text{exp}}$, whereas the minimal value of $T_e$ is $T_e(\alpha = 1.5) = 1.142 T_e^{\text{exp}}$. Therefore, the gross formula for the uncertainty of the electron temperature is

$$\Delta T_e \approx \pm 0.17 T_e^{\text{exp}} \tag{21}$$

This formula gives the maximum possible deviation of the real electron temperature from the one calculated in the planar probe model. For a thruster with $T_e = 20$ eV, the uncertainty in the measurement is 3.4 eV.

### B. Inflection Point Method

#### 1. *Operation*

The inflection point method was developed by Smith et al. [20] in an attempt to reduce the space-charge effects associated with the floating point method. Figure 10 shows an experimental emissive probe I-V trace and its derivative [20]. The inflection point of the I-V characteristic of an emitting probe in the limit of zero emission approaches the plasma potential. The inflection point is shifted slightly by space-charge effects due to emission and this shift appears to be linear (see Fig. 11) [20]. Therefore, the inflection point is measured for a number of low emission levels (temperature-limited emission on the order of electron saturation current or less) to minimize the space-charge effects, and these points are linearly extrapolated to zero emission where there are no space-charge effects.

A qualitative justification for the inflection point technique was given by Smith et al. [20]. The inflection point of a Langmuir probe I-V trace gives the plasma potential. The uncertainty of such a measurement, however, is $\sim T_e$ and can be larger if there is noise in the data. When the probe emits electrons, the inflection point is more clearly defined and easily measured with smaller uncertainties. But space-charge from the emitted electrons shift the inflection point away from the plasma potential. By extrapolating the inflection point to zero emission, the plasma potential can be accurately measured without the emitted electron space-charge effects. A more quantitative justification has recently been given [10]. Using Ye and Takamura's [28] analytical description of an emissive probe I-V trace, a theoretical emission current versus inflection point graph was

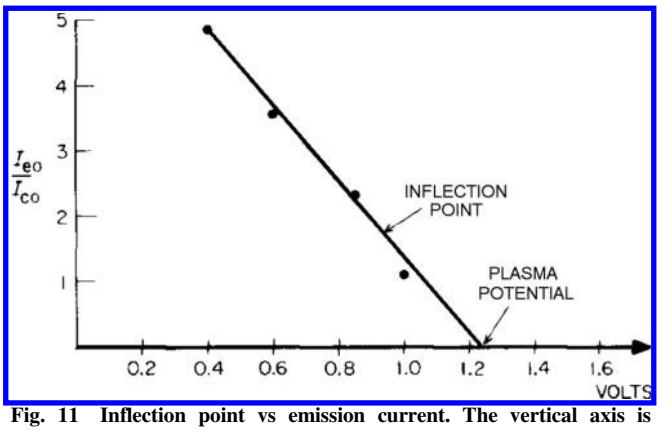


**Fig. 11 Inflection point vs emission current. The vertical axis is temperature-limited emission normalized to electron saturation current. The line fit to the inflection points is extrapolated to yield the plasma potential. (Reproduced from Smith et al. [20], with permission from AIP Publishing.)**

calculated. This analysis indicated that the inflection point method underestimates the plasma potential by $\sim T_e/10e$, but it is only qualitatively consistent with real data because of geometric effects (see the following).

The circuit diagram of the swept probe is shown in Fig. 12 [10]. A bipolar amplifier driven by a standard function generator was used to bias the probe and a floating power supply was used to heat the filament. The parameters $V_{\text{HEATING}}$, $V_{\text{PROBE}}$, and $V_{\text{CURRENT}}$ were all voltages that could be measured by a DAQ system. The voltage that drove current across the probe to heat it was $V_{\text{HEATING}}$, the potential bias on one leg of the probe was $V_{\text{PROBE}}$, and the voltage across the shunt resistor from which current could be determined was $V_{\text{CURRENT}}$. The function generator represents the driven bipolar amplifier. The isolation amplifiers are used to prevent current leakage that would affect the probe current measurements.

#### 2. *Calibration*

Determining the correct emission currents is extremely important for the inflection point in the limit of zero emission technique. Temperature-limited emission currents should be no more than a few times the electron saturation current.

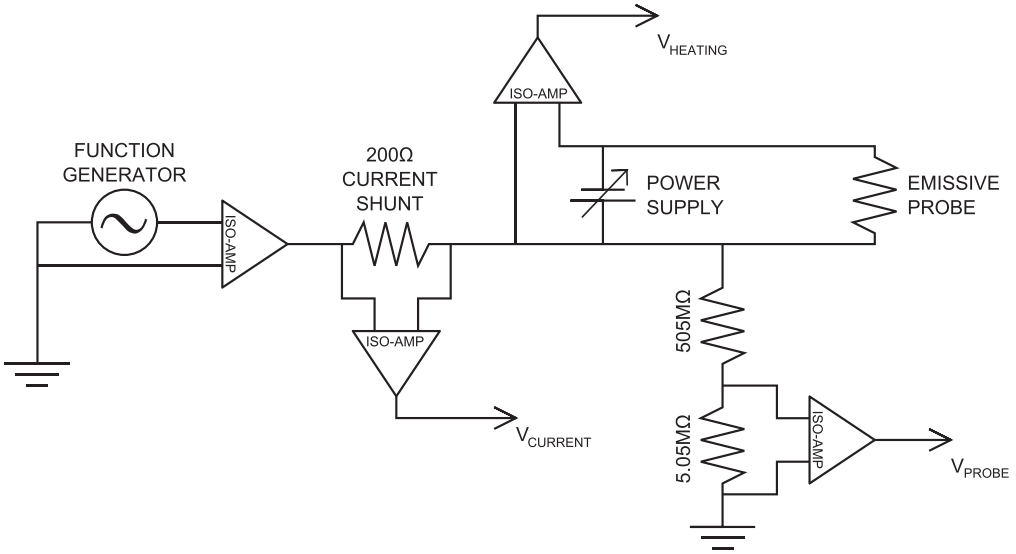


**Fig. 12 Diagram of electronics used to sweep the probe in the Hall thruster experiment. (Reproduced from Sheehan et al. [10], with permission from AIP Publishing.)**



For the most accurate measurements with this technique, the temperature-limited emission current should be less than the electron saturation current. The temperature at which the probe begins to emit sufficiently is a function of its diameter, though calculating or measuring that temperature is not critical. Only the resulting emission current is important. To determine the optimal heating so that the temperature-limited emission approximately equals the electron saturation current, heat the filament (see Sec. IV for information on heating) until it glows white hot. Incrementally increase the heating current, taking I-V traces at each heating current level until the I-V trace is modified by the electron emission. Reduce the increment and continue to increase the heating, taking I-V traces at each increment, until the temperature-limited emission current approximately equals the collected electron saturation current. The collected electron saturation current is the current at the knee of the I-V trace, just as with a Langmuir probe I-V trace, whereas the temperature-limited emission current is the current at large negative probe potentials where the current is no longer a function of bias voltage. Equation (11) provides an approximate heating current necessary. Note that this is just an approximate value. Great care should be taken when determining the ideal emission current so as not to overheat and melt the filament before any measurements are made.

To use this technique, multiple I-V traces must be taken, each with a different value of the temperature-limited emission current. At least four emission currents should be chosen, with more imparting a higher accuracy to the technique. The emission currents should be chosen to be approximately equally spaced in the range of useable emission currents.

The inflection point in the limit of zero emission technique uses an approximation that the relationship between the inflection point and the temperature-limited emission current is linear, but the true relationship is more complex. A full relationship can be calculated using a planar fluid theory and is shown in Fig. 13a [28]. The function can be divided into three regions. For the highest emission levels, the inflection point is independent of the temperature-limited emission. Just below a certain emission current, $\sim 0.028 I_{e0}$ for Fig. 13a, the relationship is approximately linear with the inflection point rising as the emission current decreases. Once the emission level is quite low, the function becomes nonlinear as the inflection point approaches the plasma potential. The inflection point in the limit of zero emission technique requires a line to be fit to this function and extrapolated to zero emission. Because only low levels of emission are used in experiments, the data points should fall in the approximately linear region. Fitting this part of the curve and extrapolating to zero yields an estimate of the plasma potential that is $\sim T_e/10e$ below the plasma potential. That scaling is independent of the plasma density. A linear fit does not capture the nonlinearity at low emission currents but the error due to the nonlinearity ($\sim T_e/10e$) is typically smaller than uncertainty due to measurement noise, so the discrepancy is minor.

Figure 13b shows the experimentally determined relationship between the inflection point and temperature-limited emission from data taken in a multidipole chamber [10,54,55]. The shape of the

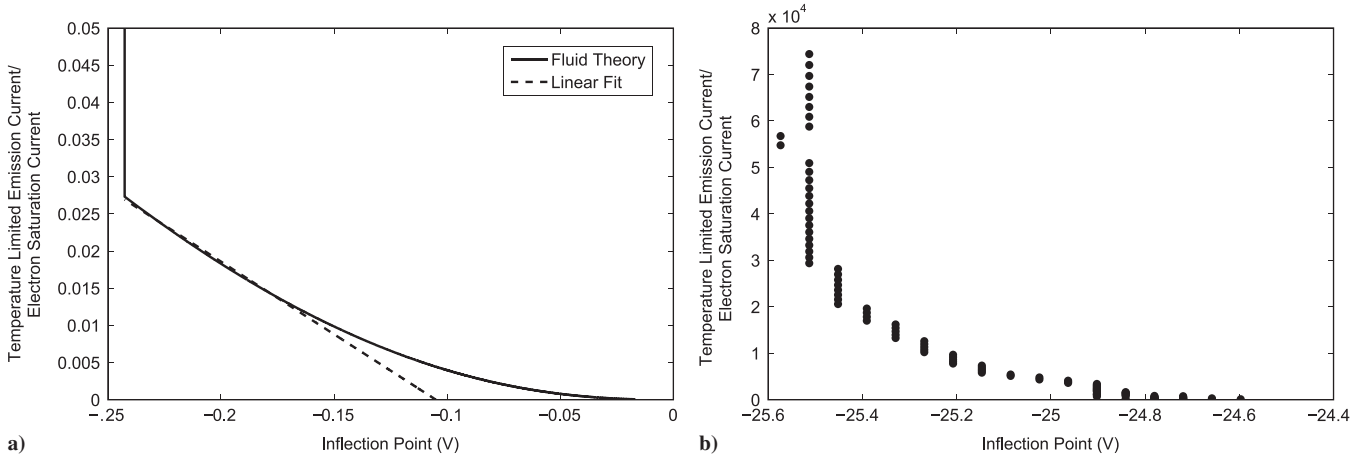


**Fig. 13 Highly detailed inflection point vs the temperature-limited emission current normalized to electron saturation current: a) fluid theory and b) data where $n_e = 1.1 \times 10^9$ cm$^{-3}$ and $T_e = 0.90$ eV.**

curve of the experimental data is almost identical to that predicted by theory, the main difference being the scale. The discretization in the horizontal axis was due to a DAQ resolution of 0.05 V. The range of inflection points is over $T_e/e$ in the experimental data, whereas in the theory is only $T_e/4e$. The biggest difference, though, is in the range of emissions in which this curve exists. The transition point between the emission independent and linear regimes occurs at $I_{et}/I_e^* \approx 0.028$ in theory, but at $I_{et}/I_e^* \approx 3 \times 10^4$ in experiments. The difference is six orders of magnitude, which is likely due to a planar theory inconsistency with a cylindrical probe. However, the accuracy of the linear fit to the $x$ intercept is unaffected by the scale on the $y$ axis.

The smaller the filament radius is relative to the debye length, the more the emitted electrons spread out compared with a larger filament, and so it takes more emission current to saturate the space charge when the probe is small. Additionally, smaller filament diameters yield larger electric fields, which permits larger emission currents. Therefore, a smaller filament affords a greater range of useful emission currents.

#### 3. *Data Reduction and Error Analysis*

The inflection point can be determined from the I-V trace by taking the maximum of its derivative. Once the inflection point versus temperature-limited emission current data points have been extracted, one only needs to fit those points to a line and extrapolate to zero emission current. The inflection point in the limit of zero emission is the measure of the plasma potential.

Noise in I-V traces manifests itself in two forms: noise in the current measurement and noise in the voltage measurement. Noise in the current can be caused by fluctuations in the plasma, a source of which cannot be reduced without altering the plasma itself. Another cause can be electrical interference if the wires connecting the probe to the measuring instruments are long. The noise in the current is most significant compared with the noise in the voltage when the current changes slowly with the bias voltage, far above or below the plasma potential. Near the plasma potential, where the probe current changes rapidly, noise in the voltage measurement is the most significant. This noise comes, principally, from noise in the electronics used to set the probe voltage. A common voltage source for I-V traces is a bipolar amplifier that can seamlessly transition from negative to positive voltages. These devices, however, tend to be quite noisy and may be unsatisfactory if very precise measurements are needed. A computer controlled DAQ system with a high-voltage operational amplifier can greatly reduce the voltage noise and lead to much better measurements.

The uncertainty of this technique is more complex than the floating potential technique. Theory predicts that it is accurate to within $T_e/10e$, which is typically less than the uncertainty from noise, so the method can be assumed to be accurate [10]. To accurately determine the inflection point, the I-V trace data must have a high enough signal-to-noise ratio for differentiation to yield a resolvable peak. If the I-V trace is too noisy, its derivative will show no clear inflection point. If the noise cannot be reduced by improving the circuit, data methods can be used. Number averaging many I-V traces in the same conditions can be time consuming but is the best way to reduce noise when taking data in a stable plasma. The I-V trace can be numerically smoothed, but too much smoothing displaces the inflection point and should not be used excessively.

The second source of uncertainty is in the extrapolation of the inflection point data to zero emission. Here it is important to take data over a wide range of emission currents. The uncertainty is the root mean square of the difference between the inflection point data and the inflection point of the fitted line at the same emission current as the data point. Note that the shortest distance from the data point to the fitted line is not the important parameter because the temperature-limited emission currents can be measured with far greater accuracy than the inflection point. The total uncertainty of the measurement, then, is the root mean square of the uncertainty in identifying the inflection point and the uncertainty from fitting the data to a line.

The uncertainty analysis of extrapolating a line fitted to uncertain data is complex. Monte Carlo simulations were performed to determine the uncertainty of the measured plasma potential $\sigma_p$ as a function of the inflection point uncertainty $\sigma_I$, the number of I-V traces $N_{\text{traces}}$, and the ratio of the maximum emission current to the range of emission currents $I_{\text{et,max}}/(I_{\text{et,max}} - I_{\text{et,min}})$. As the uncertainty of the inflection point measurement decreases and the number of I-V traces increases, the uncertainty of the plasma potential decreases. A smaller ratio of maximum emission current to range of emission currents means that the data do not have to be extrapolated as far, resulting in less total uncertainty. The empirical formula for $\sigma_p$ is

$$\sigma_p = \sigma_I \frac{2}{\sqrt{N_{\text{traces}} + 1}} \left[ \frac{3}{2} \left( \frac{I_{\text{et,max}}}{I_{\text{et,max}} - I_{\text{et,min}}} \right) - \frac{1}{2} \right] \tag{22}$$

This equation is accurate to within 5% for three or more I-V traces.

Godyak et al. [56,57] and other authors [58–60] take the inflection point of the I-V characteristic curve of a cold collecting probe to be the plasma potential. It is argued that the inflection point in the limit of zero emission is simply the inflection point with zero emission (i.e., a collecting probe). Measuring the plasma potential as the inflection point in the limit of zero emission, however, unambiguously identifies the real inflection point and linearly fitting multiple points reduces the overall uncertainty of the measurement. It has been shown that the inflection point in the limit of zero emission and the inflection point of a Langmuir probe can agree quite closely, but there are a variety of reasons to prefer the emissive probe [10]. It is difficult to identify inflection points when noise is present, so the many measurements of the inflection point in the limit of zero emission significantly reduce the uncertainty. Emissive probes can also determine the plasma potential in sheaths and plasmas with beams (see Secs. VI.C and VI.E), which is very difficult to do with a collecting probe [9].

When using the inflection point in the limit of zero emission method, it has been observed that smaller probe diameters increase the slope of the line relating emission current to inflection point [20]. The large slope leads to less uncertainty when calculating the plasma potential with this method, so smaller wires are typically preferable. Larger diameters can be useful when determining the location of the sheath edge when identifying the sheath edge by a reversal in the sign of the slope of the emission current versus inflection point (see Sec. VI.E). Most experiments have employed emissive probe wires with diameters between 0.0025 and 0.02 cm.

### C. Other Techniques

The floating point technique and the inflection point technique are the principle emissive probe methods used to measure the plasma potential in electric propulsion devices. Other emissive probe techniques exist but are, in general, not useful for electric propulsion related activities. They are briefly mentioned here to make the reader aware of them in case one is appropriate for a particular experiment.

#### 1. *Separation Point Technique*

Langmuir [1] suggested that an electric probe could be heated to a point just below emission and then, by shorting part of the circuit, temporarily increase the temperature so that the probe would be emitting. The lowest potential at which the collected current was the same for the nonemitting and emitting cases was taken to be the plasma potential. This method was improved once I-V traces could be taken because it was easier to find that point and was referred to by Chen [61] as the separation technique: If the I-V traces of the probe while cold and hot are superimposed, the point of separation is the plasma potential [62]. This simple theory, however, has been superseded by more modern analyses that consider space-charge effects and it is now known that the separation point method is unsound [10].

#### 2. *Capacitive Probe*

An option for measuring the plasma potential in high-temperature plasmas is the secondary electron capacitive emissive probe (SECP) designed by Wang et al. [63]. For the probe to have significant

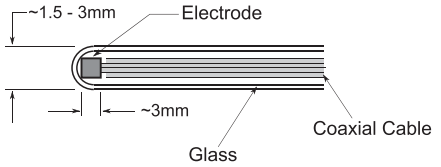


**Fig. 14 Construction of a capacitive probe. The electrode is surrounded by glass and connected to the electronics via the coaxial cable, which provides shielding. (Reproduced from Sheehan and Hershkowitz [12], with permission from IOP Publishing.)**

secondary electron emission, the material exposed to the plasma is glass, which has a secondary electron coefficient between two and three for temperatures greater than 50 eV [63]. The potential is measured capacitively by an electrode within the glass (see Fig. 14). The potential on the probe is measured across a large (~88 MΩ) resistor with a high-impedance operational amplifier as a buffer.

Because the probe is capacitive, there is a low-frequency measurement limit, which depends on the resistor and the capacitance of the cables. The typical low-frequency cutoff was 1 Hz, so this device is limited to measurements in pulsed plasmas. It was claimed that high-frequency limit is on the order of 100 MHz. Because the electrode does not float at the same potential as the surface of the glass, this probe must be calibrated before use. This was done by covering the probe with foil or dipping it in mercury and then applying a known low-frequency signal and measuring the output to determine the attenuation of the system.

A limitation to this method is that the electron temperature must be high enough to produce sufficient secondary electron emission. Experimentally, the minimum electron temperature was determined to be 20 eV [63]. If this condition is not satisfied, the SECP method yields a plasma potential significantly lower than given by the floating potential method. The benefit of this method is that the probe has a sturdy construction that is not prone to breaking or melting as other techniques are in high-temperature plasmas. The SECP method has no published use other than the first paper, so it is not known how well this technique performs in other applications, such as electric propulsion.

#### 3. *Current Bias Method*

Langmuir probes cannot be used to measure the space potential in a vacuum because there is no current to collect, yielding a structureless I-V trace. Emissive probes, however, can be used because they only emit electrons when biased below the space potential. The floating potential of an emissive probe in a vacuum, however, does not give a good measure of the space potential [64]. The vacuum current bias method was developed specifically for measuring the space-potential in a vacuum with no plasma. Usually, when taking an I-V trace, the voltage on the probe is applied and the current measured. The vacuum current bias method fixes the current drawn from the probe and the voltage of the probe is measured instead [65]. The emissive probe is first placed in a known space potential. The probe is biased to that known potential and the emission current is measured. The space potential can be determined in other locations by the potential at which the probe emits the same emission current as was measured in calibration. Although it is possible to use the current bias method to measure the plasma potential [65], it essentially reduces to the floating potential technique and, therefore, it will not be discussed it in further detail.

### D. Method Comparisons

It has been observed that the various emissive probe techniques do not agree with each other [10,20,38]. Typically, the floating point method gives a lower measure of the plasma potential than the inflection point method. A dedicated study regarding this question was performed in a Hall thruster plasma with electron temperatures between 10 and 50 eV [10]. The probe location was 0.5 cm away from the face of the thruster and between 0 and 0.2 cm radially inward from the outer channel wall. By varying the discharge voltage, the acceleration region position changed and thus the

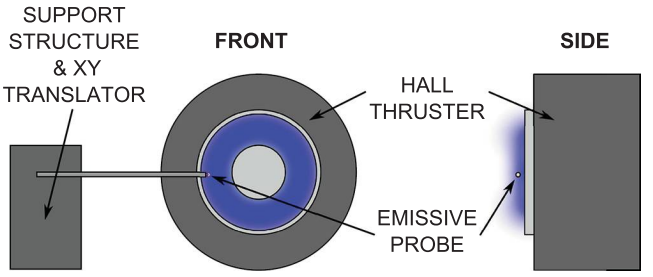


**Fig. 15 Schematic of a typical emissive probe on a 2-D translation stage to measure the plasma potential in a Hall thruster.**

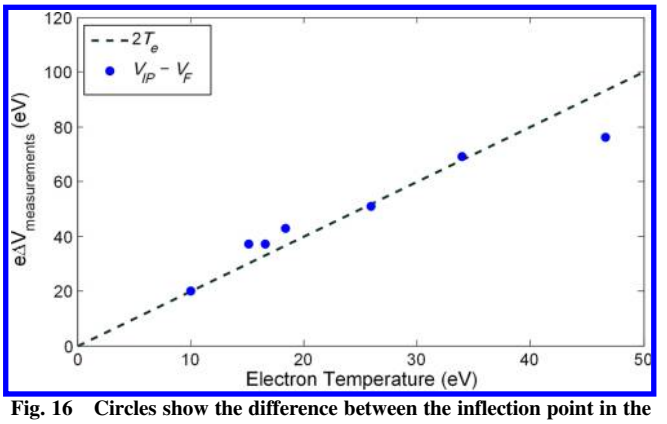


**Fig. 16 Circles show the difference between the inflection point in the limit of zero emission technique. The dashed line is a reference line indicating where a difference of $2T_e/e$ would fall.**

electron temperature varied. Figure 15 shows the probe mounted to a two-dimensional (2-D) motion table to control its position.

Figure 16 shows the difference between the inflection point method and the floating point method [10]. The comparison between the techniques shows that the inflection point method yields a value $\sim 2T_e/e$ above the floating point method, which is fairly consistent with the $1.5T_e/e$ predicted from fluid theory and particle-in-cell (PIC) simulations [2,44]. The authors conclude that the inflection point in the limit of zero emission more accurately measures the plasma potential than the floating point method. The floating potential technique is predicted by fluid theory to yield a measure of the plasma potential $\sim 1.5T_e/e$ below the plasma potential, whereas the inflection point technique is predicted to yield a measure $\sim T_e/10e$ below the plasma potential. The data are consistent with these predictions, though a comparison of emissive probes to another method for determining the plasma potential (such as laser induced fluorescence) would be more definitive.

Although the inflection point technique may be the most accurate, it is not the best technique for every experiment (see Sec. VII). The inflection point method cannot measure temporal variations easily and in high-energy density plasmas there is a greater risk of failure. If the electron temperature is small, the difference between the inflection point technique and the floating point technique will be small as well. Additionally, if the electron temperature is constant, the floating point technique's error is constant, and so relative changes in the plasma potential and electric field measurements will still be correct. The authors suggest that the floating point method be compared with the inflection point in the limit of zero emission method before use, though, to ensure the measurements will be accurate.

## IV. Heating Methods

Most emissive probe designs require the probe to be heated to the point where it begins emitting electrons. There are several ways to do this and each method has its own strengths and weaknesses.

### A. Direct Current Joule Heating

The most common method for heating an emissive probe is to simply run current through it. This method is easy to control by varying the current and can be most simply implemented with a continuous direct current. There is a distribution of bias voltages across the filament because a potential drop (the heating voltage $V_H$) is required to make current flow. A good approximation of the effective bias potential is the potential at the hottest part of the probe because electron emission is highly temperature dependent [see Eq. (7)]. Because the ends are cooled by conduction to the supports, the middle of the probe is the hottest part. Therefore, the effective bias voltage can be taken as the bias potential at the middle of the probe [62]. Depending on the heating circuit, this could mean that the effective bias potential is the bias potential plus $V_H/2$, 0, or $-V_H/2$ [66].

Thermionic emission for thoriated tungsten occurs at appreciable current densities around 2000°C. At these temperatures, emissive probes are fragile and prone to early failure due to evaporative mass loss, thermal shock, and, above all, human error. In the simplest case, probes may be heated manually from a power supply front panel control, especially for robust wires of 0.5 mm or larger diameter. However, for finer wire, a computer-controlled heating profile with a linear ramp to emission from a warm "idle" state is recommended. The heater power supply must be floated with respect to ground and it is important to ensure that the maximum allowable floating potential is greater than the expected plasma potential. If the power supply attempts to float at a larger voltage than it can tolerate, then the current can find additional paths to ground through the power supply, leading to significant error. Typical power supplies tolerate 25–40 V floating potentials, but some can handle as high as 500 V.

Several factors motivate keeping the probe at a warm idle current when not actively taking a measurement. Because of evaporative mass loss, one should minimize time at emissive temperatures. However, filament failure from thermal shock in hot–cold cycling is a risk for small filaments. An emitting filament cooled to ambient temperature may fracture along recrystallized grain boundaries as it cools, even under carefully controlled cooling. Instead, a convenient idle current level is the heating current where the probe has just become visibly red hot. Once a filament has been heated for the first time, it is best practice to return to the warm idle between measurements and continue testing until probe failure, rather than allow the filament to cool completely. A warm idle also keeps the probe body closer to thermal equilibrium, making it easier to identify the heating power that produces saturation without overshooting during the slight delay between applying a heating current and the probe temperature response.

For smooth, reproducible fine control without human error, a computer-controlled heating circuit used with good success in the interrogation of Hall thruster discharges is shown in Fig. 8. A programmable power supply with remote current control capability was driven by an analog voltage source with a unity gain isolation amplifier to float the analog control voltage. The analog voltage was ramped by software such as LabView over a USB interface and the power supply output current was calibrated to the analog inputs. This enabled smooth, repeatable linear ramping of the heating current from idle to saturated emission, with built-in delays for data acquisition at peak current. Based on the authors' experience, for a 0.1-mm diameter filament, the warm-idle current may vary between 1.5 and 2.5 A due to variations in probe construction, with the emitting current generally 0.3–0.5 A higher. A detailed expression of the probe temperature as a function of heating current can be found in Eq. (11), but unknowns in the experimental setup make experience more valuable. Initial experiments should use the procedures described in the calibration section of the appropriate technique (described in Secs. III.A.2 and III.B.2). A typical heating schedule, used successfully, though not optimized, is a 10–20 s ramp time from idle to emission with a pause at peak heating of 2–3 s before data acquisition.

### B. Alternating Current Joule Heating

For more accurate knowledge of the bias potential, measurements can be taken while there is no voltage drop across the filament [42].

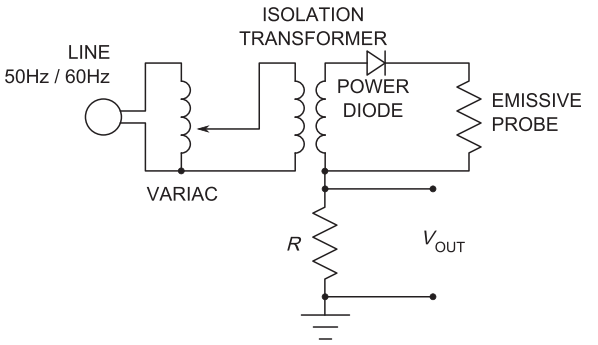


**Fig. 17 Half-wave rectifier used to heat and measure the current from an emissive probe.**

To do this, the filament must be heated with half-wave rectified alternating current and the data taken during the nonheating half-cycle. A simple example of a circuit for this purpose is shown in Fig. 17 [41]. Outlet power at 50 or 60 Hz is often used, but higher frequencies can be used as well [67]. Care must be taken that the I-V trace is recorded quickly with respect to the cooling time of the probe (typically on the order of 10 ms) when using ac heating in conjunction with the inflection point method. Fujita et al. [42], using a 0.5-mm diameter wire, showed that the inflection point can change by up to 1 V during the off cycle due to cooling, though the floating point did not vary during the off cycle.

### C. Self-Emission

High densities and temperatures make probe use more complicated. The probes themselves can perturb the plasma, the shaft can introduce impurities, and the high-energy density can cause the probe to melt [57,68]. The melting problem is especially acute in emissive probes when using joule heating and taking I-V traces. The heating required to bring the probe to high emission is frequently enough to melt the wire. These problems can be reduced by using a self-emitting probe, which is heated to emission by the energy in the plasma itself, a technique designed by Hershkowitz et al. [68]. A self-emitting probe consists simply of a wire end exposed to the plasma. The electronics for measuring the probe current are a resistor or high-impedance operational amplifier connected from the probe to ground, across which the voltage can be measured; the floating point technique is the underlying method for self-emitting probes. Because there does not need to be a closed wire loop through which current can pass, the supporting shaft size can be smaller, reducing impurities and perturbations. To date, self-emitting probes have only been used at the edge of magnetically confined fusion plasmas ($T_e \approx 30$ eV, $T_i \approx T_e$, $n_e \approx 3 \times 10^{13}$ cm$^{-3}$) [68–70]. However, these conditions suggest that self-emissive probes may be successful in high-energy density electric propulsion plasmas such as arcjets, magnetoplasmadynamic thrusters, or Hall thruster channels, which, in some cases, are only somewhat less hot and dense.

It takes time for the probe to be heated to emission, a few milliseconds, generally, and so the plasma potential during heat up cannot be known. The equation governing the probe heating is

$$\frac{1}{2}\frac{ek_B n_e(v_i T_i + v_e T_e)}{C_p a \rho} = \frac{\Delta T_w}{\Delta t} \tag{23}$$

where $v_\alpha$ and $T_\alpha$ are the thermal velocity and temperature of species $\alpha$, $C_p$ is the specific heat of the probe material, $a$ is the radius of the probe, $\rho$ is the density of the probe material, $T_w$ is the probe temperature, and $t$ is time [68]. This equation assumes that energy losses from the probe were small compared with the gains to it, which is true for most pulsed fusion experiments. It is clear from this equation that, if the density and temperature of the plasma are too large, the probe will heat up too quickly and melt in the course of a single shot. Therefore, if the density and temperature are too high, the radius must be increased to prevent melting. How large of a radius perturbs the plasma significantly depends on the specifics of the

experiment. To prevent the probe from being destroyed, it can be quickly inserted into the plasma of interest and back out before it melts. Rohde et al. [69] used a pneumatic drive to move the probe at 1 m/s, allowing potential measurements to be made in a plasma where $T_e = 80$ eV and $n_e = 2 \times 10^{13}$ cm$^{-3}$. Similar measurements were successfully made by Fink et al. [70].

Another limiting factor is that the electron emission current must be larger than the electron collection current for the floating potential to be a good indicator of the plasma potential [68]. Starting from the conditions that the emission current is greater than the collected current and the probe is heated to just below the melting point, a limitation based on the density and temperature for which a pure tungsten self-emissive probe can survive can be derived:

$$n_e < \frac{1.8 \times 10^{14}}{\sqrt{T_e}} \tag{24}$$

where $n_e$ is in cubic centimeters and $T_e$ is in electron volts.

### D. Laser Heating

Although the aforementioned heating schemes are simple and easy to employ, there are serious drawbacks to each. Running current through the filament causes many problems due to the bias voltage and temperature distributions across it. The laser heated method provides a solution to these problems, though involving a more complicated setup. Ono and Teii [71] developed a system by which a probe was heated to emission via an infrared laser and I-V traces were taken. The laser was a 10–20 W continuous wave $CO_2$ laser directed at a 0.4-mm diameter sphere of platinum, coated with carbon to improve the absorption of the laser energy. By changing the power of the laser, different levels of emission could be reached.

This scheme has been applied in dc discharges [71], RF discharges [72,73], and tokamaks [30]. The probe itself can be made of a variety of materials, including platinum, tungsten, graphite, and $LaB_6$. The greatest benefit of heating with a laser is that there is no potential distribution across the probe. Because of this, laser heated probes have attracted attention from the fusion community in recent years [30,74–77]. Particularly noteworthy is the movable laser heated emissive probe designed by Schrittwieser et al. [74], as shown in Fig. 18. This design allows the probe to be moved without needing to refocus the laser and has been employed in a helicon discharge. A study of various probe materials for laser heated emissive probes indicates that a graphite tip causes the least noise in the measurements, but $LaB_6$ emits more current for a given laser power [77,78]. Additionally, it was found that $LaB_6$ is extremely robust, showing no signs of evaporation even after hours of continuous heating, giving it a much longer lifetime than a tungsten probe. All of these factors combine to make a laser heated probe a promising technique for high-energy density plasmas.

## V. Probe Construction

The design scheme of an emissive probe can significantly affect the performance and lifetime of the probe. A number of common designs are presented in this section to apply to a variety of types of plasmas.

### A. Material

In many cases, emissive probes are made out of tungsten. Tungsten has the highest melting point of any metal (3695 K), which allows it to be heated to higher temperatures and greater emission than other metals [79]. Frequently, the tungsten is doped with thorium oxide, usually at between 0.5 and 2.0%, which increases the electron emissivity by up to three orders of magnitude by reducing the work function of the wire. Thorium is radioactive but is an alpha emitter, so it is not dangerous unless ingested. The thorium oxide is initially present throughout the tungsten, but after heating, it diffuses to the surface, a process studied in detail by Langmuir [80]. Thoriated tungsten emissive probes have been employed in a wide range of plasmas from vacuum [64] to tokamaks [81]. It is the most commonly used emissive probe material for measurements in electric propulsion devices. Tungsten and thoriated tungsten are convenient choices for constructing emissive probes in any plasma that does not contain oxygen. When using a laser heated emissive probe, however, a wider variety of materials are available, so graphite or $LaB_6$ can be used (see Sec. IV.D).

Typically, when using a wire as an emissive probe, the wire diameter should be kept as small as possible. This is to minimize the disturbance to the plasma and the heating current needed to heat the wire to emission. Most experiments have employed emissive probe wires with diameters between 0.0025 and 0.05 cm. There are, however, other considerations to keep in mind. Higher heat fluxes in high-energy density plasmas can melt thinner wires, whereas thicker ones can conduct away sufficient heat to survive [68]. When studying plasmas produced by plasma thrusters, magnetrons, and other devices with ion flows, sputtering can severely limit the probe's lifetime, so thicker wires may be used to allow the probe to survive longer [24].

Probe lifetimes in electric propulsion devices can range from seconds to tens of hours, depending on the plasma conditions. Overheating is a major issue for probes in high-energy density plasmas, such as the Hall thruster channel, where the particle flux to the probe is so large that the probe can melt. These regions can be probed with high-speed (several meters per second) translation stage

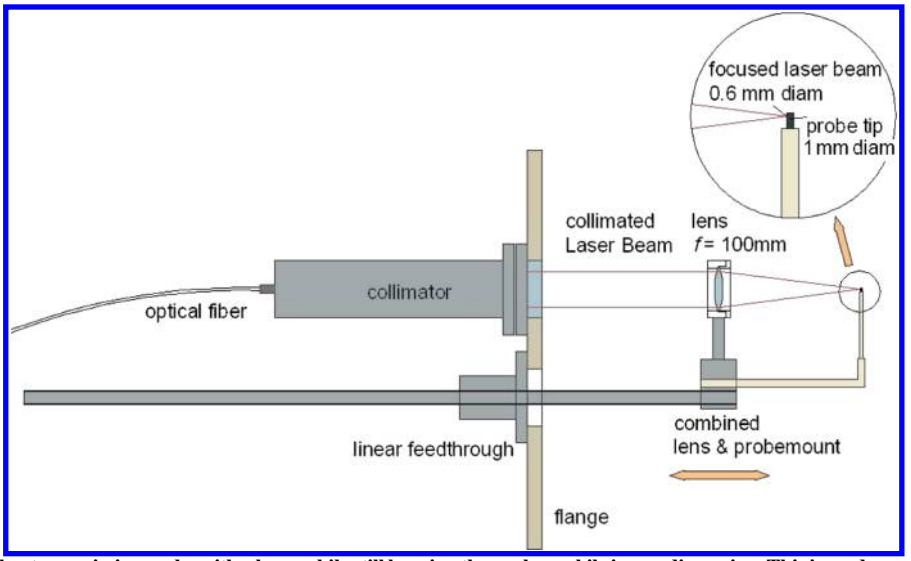


**Fig. 18 Scheme used to heat an emissive probe with a laser while still keeping the probe mobile in one dimension. This is made possible by the lens mounted on the linear feedthrough, keeping the distance from the lens to the probe constant. (Reprinted from Schrittwieser et al. [74] with permission.)**

so that the probe can be inserted, measurements taken, and removed again before it is destroyed [82]. Ion sputtering is the major issue in the plume. Xenon ions with energies of ∼1200 eV have a sputter yield (number of sputtered atoms per incident ion) of tungsten of ∼1.7 [83–85]. If an ion engine were producing a beam current density of 1 $\mathrm{mA/cm^2}$, a probe in the beam would have a sputter rate of $1 \times 10^{-7}$ cm/s. A probe with radius 0.01 cm would last for approximately 25 h, neglecting other lifetime limiters such as evaporation and stresses from heating. The use of positioning setups and limited exposure of the probe to the plasma is important to implement to extend the probe lifetime. With careful technique (not over heating the probe, moving the probe out of the beam when not in use) a lifetime of 10 h can be achieved.

### B. Shape

Various schemes have been devised to secure the tungsten wire electrically and mechanically. It is critical that the emissive probe be secured in a manner that holds the probe in place while letting it be exposed to the plasma. If there is too much insulator next to the probe, the insulator can become charged from the emission and distort the local plasma potential. There are two different designs for exposing the wire to the plasma. The most common design for joule heated emissive probes is a hairpin loop, as shown in Fig. 1 [14]. This is a convenient design because it simply requires connecting the emitting wire to the wire leads (see Sec. V.C) and pulling the leads into a ceramic tube so that only the emitting wire is exposed. For a hairpin loop, the filament length (which determines the distance from the emitting point of the filament to the ceramic) should be $>2\lambda_d$ so that the ceramic's sheath does not overlap the emissive probe sheath and affect the plasma potential measurement [86]. The limitation of this design is that the probe is not purely cylindrical, as is assumed when taking I-V characteristics. Space-charge and geometric effects near the bend in the wire due to overlapping sheaths from different points of the filament can become significant when the debye length is on the order of the radius of the bend [14], which can occur in conditions of thruster plumes.

For a more accurate indication of the plasma potential at low densities when the space-charge effects are significant, a linear emissive probe should be used (see Fig. 19). This design is more difficult to construct, but does lead to more accurate plasma potential readings in low densities. Because the linear design only has significant extent in one dimension, the position is better defined and spatial resolution is improved over the hairpin design. Kemp and Sellen [14] showed that, in a plasma with $T_e \sim 1$ eV and densities on the order of $10^6$ $\mathrm{cm^{-3}}$, the plasma potential measured by a hairpin probe is 0.2 V lower than that measured with a linear probe, a difference that gets worse at lower densities. It is important when building this version of the emissive probe to give the wire a slight amount of arc. The physical distortion of the probe caused by heating and cooling and the brittleness of a hot probe will break a taut filament after a single use.

Emissive probes that do not rely on joule heating can have a smaller probe and smaller support structure if no current need be run through the wire. Self-emissive probes merely require a small end (2 mm) of the emitting wire exposed to the plasma and otherwise protected by an insulating tube [68]. Laser heated probes, too, avoid the problems caused by joule heating and can be made in an arbitrary shape [72].

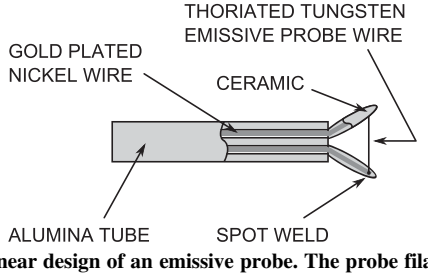


**Fig. 19 Linear design of an emissive probe. The probe filament is the only conducting part exposed to the plasma; all else is insulated with ceramic. (Reproduced from Sheehan and Hershkowitz [12], with permission from IOP Publishing.)**

### C. Connection

Connecting a tungsten wire to wire leads is a nontrivial problem. Although there have been reports of tungsten being soldered with silver or copper, it required temperatures in excess of 1100°C and soldering time of 1–15 min, which is often not practical [87]. One solution is to spot weld the tungsten wire to gold plated nickel wires and then solder those to the appropriate connections [14]. Nichrome (nickel-chromium) wire has been used as an alternative to gold plated nickel [88]. To reduce the current requirements of heating the probe, Motley [89] made a tapered filament by electrolytically etching the exposed part of the wire. A 0.025-cm diameter tungsten wire was used to construct a typical hairpin loop. That loop was dipped in sodium hydroxide solution to etch the tip of the wire, reducing its diameter to 0.005 cm. only at the tip. Others forgo the spot welding and simply use the mechanical contact created by squeezing the filament and connecting wire into the bore of the ceramic tube to maintain good electrical contact [90]. Siebenforcher and Schrittwieser [91] employed a variation of this design where the filament was braided into the connecting wire for a more secure contact. Finally, the filament may be inserted into small copper tubes of the type used in electric discharge machining with care to keep the hot tip far enough from the junction to avoid melting the copper [43].

### D. Support Structure

The basic support structure for most probes, including emissive probes, is a series of progressively smaller tubes, making a so-called telescoping probe [15]. The end tube is typically a dual bore alumina tube to isolate the two legs of the emissive probe (see Fig. 19). Alumina is typically the material of choice because it is low cost, a good insulator, and can withstand high temperatures (up to 2000 K). Most probes for low-temperature plasmas can be made with alumina supports. Alumina can, however, trap vapors during machining processes that can outgas when the alumina is subjected to vacuum. This does not make alumina unusable in vacuum applications, but it is important to make sure that tubes are well outgassed before their application in plasma. Outgassing can be achieved by placing the probes in vacuum until the vacuum chamber reaches the base pressure achievable when no alumina is in the vacuum chamber.

There are some cases, however, when alumina cannot or should not be used. In destructive plasmas with sufficiently high-energy density, the alumina can be quickly ablated due to plasma heating that can be enhanced if plasma electrons are hot enough to induce a strong secondary electron emission (SEE) [82]. Just like emissive probes, the increased heating of the probe structure is due to reduction of the sheath potential. For alumina ceramic, the SEE yield reaches a critical value of one at lower energies than for boron nitride ceramics. Apart from heating of the tube, SEE can introduce serious perturbations to the local plasma potential due to colder SEE electrons injected into the plasma. This is especially relevant to plasmas with magnetic fields, such as in many electric propulsion devices. Staack et al. [7] investigated probe support structure materials and designs in a Hall thruster where probes with an alumina tube modified the discharge current by a factor of 2. They found that using a conductive shielding around the alumina greatly reduced the secondary electron emission, but allowed current to be transported from one end of the support to the other, shorting the plasma. To solve this, they designed a support tube with segmented conductive shielding, which effectively reduced secondary electron emission while not short circuiting the plasma. The segmented shields were made by either plasma spray coating alumina with tungsten and then machining the tungsten into rings or by cementing short graphite rings onto the alumina tube (see Fig. 20) [7]. Note that the segmented rings must be robust. Simpler designs with graphite paint applied over tubes have seen the conductive surface sputtered away during insertion into a Hall thruster discharge channel. Using the segmented shield reduced the plasma current perturbation to 4%. Both designs functioned effectively.

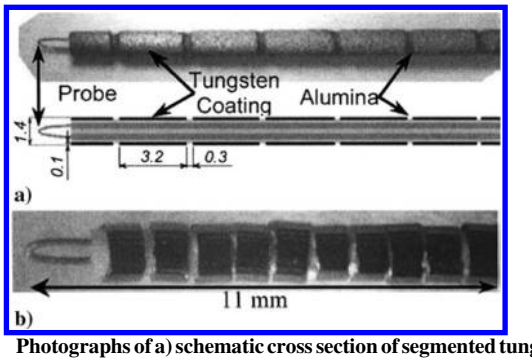


**Fig. 20 Photographs of a) schematic cross section of segmented tungsten probe, and b) segmented shield using graphite ringlets (dimensions in millimeters). (Reproduced from Staack et al. [7], with permission from AIP Publishing.)**

### E. Probe Insertion into Plasma

#### 1. *Movable Probes*

It is possible to make plasma potential measurements while the emissive probe is moving if the floating point technique is used [3,69]. Rapidly moving the probe into and out of the plasma may be necessary in harsh plasma conditions that do not permit a long lifetime of the probe. Linear actuators can move probes on the order of 1 m/s with 10 $\mu$m precision [82]. In these cases, the limit on position knowledge is the probe vibration due to the rapid acceleration, which is difficult to quantify without high-speed photography.

Rapid insertion of emissive probes into high-energy density plasmas can cause thermal shock and fracture of alumina tubes, reducing the lifetime of the probe. Boron nitride (BN) has a higher thermal conductivity, so coating the alumina with BN can significantly increase the lifetime. Probe methods that rely on I-V traces should not be used while the probe is moving because the data will be convolved over a range of positions, unless the sweeps are sufficiently fast to achieve many sweeps with a desired spatial resolution. Recent work with rapidly swept Langmuir probes suggests this may be possible with emissive probes as well [40]. Alternatively, it may be possible to fix the probe at a potential and measure the current as a function of time as the probe is inserted into the plasma. If this is repeated for many probe biases and the plasma is unchanging, a set of I-V traces as a function of position could be constructed. The authors are not aware, however, of any experiments using this technique.

#### 2. *Probe-Induced Perturbation of the Plasma*

The presence of a probe in a plasma inevitably introduces perturbations. Probes and their supporting structures are loss surfaces that can change the dynamics of a discharge. Emissive probes in particular also add electrons back into the plasma with a different distribution function than that of the electrons that were removed. The floating potential method is particularly susceptible to causing that perturbation because it relies on large emission currents. Keeping the emitting filament small reduces the total emission current into the plasma and can help to minimize any problems caused by the emitted electrons.

Experiments on a Hall thruster have shown that secondary electron emission from the probe support structure can have a significant impact on the discharge [7]. For a constant anode potential, the discharge current can change by up to 30% depending on the position of a probe supported by an alumina shaft. Additionally, energetic ion bombardment of the alumina will cause it to ablate, limiting the lifetime of the probe, though this is rarely the lifetime limiting mechanism, due to the fragility of most filaments. SEE was determined to be the primary cause of the disruptions because coating the support structure with low-SEE material was found to greatly reduce these effects, as was mentioned in Sec. V.D.

## VI. Special Cases

Although the principle of emissive probes is the same in every plasma, there are special cases that warrant more detailed examination. The following sections describe the particular way in which emissive probes are applied to each specific system.

### A. Plasma Thrusters

Emissive probes have been used in many types of electric propulsion devices, though more so in Hall thrusters and helicon thrusters than other types. Table 1 shows representative electron density $n_e$, electron temperature $T_e$, debye length $\lambda_d$, ion-neutral mean free path $\lambda_{i-n}$, and electron Larmor radius $r_{L,e}$ for different locations in arcjets, Hall thrusters, helicon thrusters, ion engines, magnetoplasmadynamic (MPD) thrusters, and pulsed plasma thrusters (PPT) [92–99]. Note that these numbers are only meant to be interpreted as examples from particular thrusters as a point of reference for determining the importance of the various effects described in this article. There can be great variation of these values between thrusters and before an emissive probe is used to measure the plasma potential in a particular thruster the specifics of that thruster must be considered.

The arcjet throat, Hall thruster channel, and MPD all have high-energy densities that can easily destroy probes, making high-speed translation stages necessary. The PPT has a high density, but it is a transient plasma without enough energy to destroy a probe. In most cases, the Debye length is much smaller than the probe diameter, so planar sheath theory can be used, though low densities in the Hall thruster and ion engine plumes may result in finite sheath size effects [31]. The ion-neutral mean free path is typically very long compared with the probe size, so the presheath length is determined by the probe size [100]. An electron Larmor radius smaller than the probe will make the effective probe area smaller, though magnetic fields are typically not large enough for that to happen.

In Hall thrusters, extracting an accurate measurement of the plasma potential profile and, relatedly, electric fields in the acceleration region from floating emissive probe data is nontrivial. Basic emissive sheath theory predicts that the large electron temperatures on the high potential side of the acceleration region will cause correspondingly large errors in the plasma potential measurement. The electron temperature drops through the acceleration region, resulting in a variation of error in those

**Table 1 Representative plasma parameters in a variety of thrusters**

| Thruster (location) | Gas | $n_e$, cm$^{-3}$ | $T_e$, eV | $\lambda_d$, cm | $\lambda_{i-n}$, cm | $r_{L,e}$, cm | Source |
|---|---|---|---|---|---|---|---|
| Arcjet (throat) | $H_2$ | $8 \times 10^{13}$ | 1.9 | $1 \times 10^{-4}$ | $1 \times 10^{5}$ | 0.5 | [92] |
| Arcjet (plume) | $H_2$ | $1 \times 10^{11}$ | 0.4 | $1 \times 10^{-3}$ | 100 | 5 | [92] |
| Hall (channel) | Xe | $1 \times 10^{13}$ | 30 | $1 \times 10^{-3}$ | 1 | 0.2 | [93] |
| Hall (plume) | Xe | $1 \times 10^{11}$ | 1 | $2 \times 10^{-3}$ | 2000 | 0.8 | [94] |
| Helicon (throat) | Xe | $1 \times 10^{11}$ | 5.5 | $6 \times 10^{-3}$ | 10 | 0.06 | [95] |
| Helicon (plume) | Xe | $1 \times 10^{9}$ | 5.5 | $6 \times 10^{-2}$ | 20 | 1.8 | [95] |
| Ion (discharge) | Xe | 0.174 | 3.5 | $6 \times 10^{-3}$ | 10 | 0.7 | [96] |
| Ion (plume) | Xe | $1 \times 10^{9}$ | 1 | $2 \times 10^{-2}$ | 200 | 7.6 | [96] |
| MPD (throat) | Ar | $2 \times 10^{15}$ | 3 | $3 \times 10^{-5}$ | 0.006 | 0.007 | [97] |
| MPD (plume) | Ar | $1 \times 10^{14}$ | 1.5 | $9 \times 10^{-5}$ | 20 | 1 | [97] |
| PPT (max) | Teflon | $1 \times 10^{15}$ | 2 | $3 \times 10^{-5}$ | 200 | 0.005 | [98,99] |

measurements with respect to position in the acceleration region [36]. The plasma potential as measured by the floating potential technique will result in a monotonic potential drop across the acceleration region. If, however, the potential measurements are adjusted by $1.5T_e/e$ when the electron temperature is not constant, the plasma potential can be nonmonotonic with a bump in the potential distribution just before the acceleration region [34,101].

There is disagreement in the community on whether this bump is physical or nonphysical. Because the anode sheath is predicted (and measured) to be negative, there can be a situation with a virtual anode formed in front of the anode. The potential bump could be as high as $\sim T_e/e$. This bump is essentially a result of the pressure gradient that has a peak in front of the acceleration region. This explanation, however, has not yet been quantitatively validated by model, leaving open the possibility that there is an error in the $1.5T_e/e$ adjustment. On the other hand, not adding any correction to the floating potential measurements is not correct due to the emissive sheath potential. Both approaches, adding a correcting factor and not adding a correcting factor, have issues due to absence of good modeling validation.

Multiple complicating factors may cause a simple $1.5T_e/e$ adjustment of the measured plasma potential to fail. When making measurements within the channel of the Hall thruster, where the walls are typically within 10 cm of the probe, the presheath can introduce an error to the measurements. A presheath surrounds the emissive probe sheath, just as with a collecting probe, to accelerate ions. The length of the presheath is determined by collisional effects, making the presheath size on the order of the ion-neutral mean free path [102], or geometric effects making it on the order of 10 probe radii (typically ~1 mm for emissive probes) [31], whichever is smaller. When boundaries are within two presheath lengths of the probe, the presheath can be determined by the distance between the probe and the wall. To date there have been no measurements that have been made so close to the wall of an electric propulsion device that the presheath is modified, so it is unknown how that would affect measurements.

Additionally, the Hall thruster plasma is predicted to have a non-Maxwellian EEDF [103]. For example, under conditions of a bi-Maxwellian EEDF with cold and hot electrons, a simplified picture is as follows. The presheath potential drop depends on the electron temperature of less energetic electrons trapped in quasi-neutral plasma, whereas the sheath potential drop is governed by energetic electrons, which can overcome the sheath potential barrier and get to the wall. However, for Hall thrusters, the situation could be more complicated due to predicted anisotropy of electrons with different velocity distribution functions across and along the magnetic field [104]. In addition, secondary electrons from the thruster channel walls make up a second electron population with a different average energy in the plasma. Therefore, the energy distribution function may vary in the acceleration region. Overall, for plasmas with non-Maxwellian electrons, it is not always straightforward what electron temperature should be used for estimating the temperature adjustment of the floating potential of the hot probe due to the space-charge saturated sheath. The importance and quantitative effects of the presheath, secondary electrons, and distribution function continues to be an active area of research. No quantitative answers to these questions, such as how large is the presheath potential in a Hall thruster, have yet been obtained. For this reason, a simple $1.5T_e/e$ correction to the floating potential method's measurement of the plasma potential cannot be made.

### B. Magnetic Fields

Emissive probes can be used in plasmas with magnetic fields [24,38,81,105,106]. A probe emitting in a magnetic field has a modified effective probe area because electrons emitted perpendicularly to the field will be trapped in gyromotion and unable to escape and be emitted. This should not be a significant effect unless the probe wire is oriented along a magnetic field line, in which case almost none of the emitted electrons could escape. Therefore, for emissive probe measurements in the magnetic field, the probe should be placed in such a way that the magnetic field lines intersect the probe filament (i.e., the probe filament orientation is perpendicular to the magnetic field).

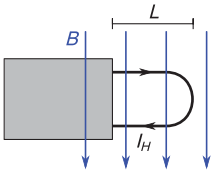


**Fig. 21 Hairpin emissive probe in a magnetic field.**

If the magnetic field is strong enough, a filament can be deformed due to the force resulting from the current passing through it, as in the case of the Joule heating method, though the magnetic fields in electric propulsion devices are typically not strong enough to do this [74]. Consider the case of a hairpin loop probe in a magnetic field, as shown in Fig. 21. Euler–Bernoulli beam theory with uniform loading can provide an order of magnitude estimate of the displacement, where one side of the probe would attempt to displace into the page and the other out of the page. The displacement $\delta$ with a uniform load is

$$\delta = \frac{I_H B L^4}{8EI} \tag{25}$$

where $I_H$ is the heating current through the probe, $B$ is the magnetic field strength, $L$ is the length of the probe, $E$ is Young's modulus, and $I$ is the area moment of inertia based on the wire cross section. Worst-case values in a Hall thruster might be $I_H = 2$ A, $B = 200$ G, $L = 0.5$ cm, and $I = \pi r_p^4/4 = 1.2 \times 10^{-9}$ cm$^4$ with a 0.0125-cm diameter filament. Young's modulus for tungsten is 411 GPa at room temperature, but drops to ~300 GPa at emissive temperatures [107]. In this case, the displacement is only $\sim 10^{-4}$ cm. If, however, a 0.005-cm diameter filament was used in a magnetic field of 20,000 G, such as in the variable specific impulse magnetoplasma rocket (VASIMR) [108], the displacement would be ~3 cm, larger that the size of the probe and resulting in the probe being distorted to the point of destruction. The displacement should be approximately less than a filament diameter to ensure that distortion from the magnetic field is not significant. Laser heating avoids this problem because there is no heating current and recent work has centered around this heating method [30,73,74,76–78].

### C. Double Layers and Beams

Emissive probes are especially useful in the presence of double layers and beams [9,109,110]. Double layers are stationary electrostatic shock-like structures that have a rapid spatial transition ($\sim 10\lambda_d$) from a high potential to a low potential [109]. Double layers can be formed with currents, but current-free double layers (CFDLs) have gained attention lately for application in helicon plasma thrusters [111,112]. Helicon plasma thrusters are a class of electric propulsion under development by a number of groups that uses radio frequency helicon waves to heat electrons, which ionize the propellant [95,113–115]. That plasma expands out of the thruster through a diverging magnetic field, which functions in a similar way to a conventional rocket nozzle. A neutral beam forms, consisting of a jet of ions and electrons, without need for a neutralizing cathode. CFDLs have been observed to be one of the possible ion acceleration mechanisms [116,117], with ambipolar ion acceleration being the other [118]. It is important to note that, although CFDLs are predicted to produce no thrust [119], experiments have shown that diamagnetic forces in these systems contribute significantly to the thrust [120].

In double layers, streams of ions and/or electrons can make collecting Langmuir probe traces difficult to read because collecting probes do not distinguish between potential and kinetic energy. Emissive probes, though, only start emitting electrons at the plasma potential, making it the preferred diagnostic for measuring potential in double layers and beams [121]. Figure 22 shows measurements from a helicon plasma source expanding through a magnetic nozzle

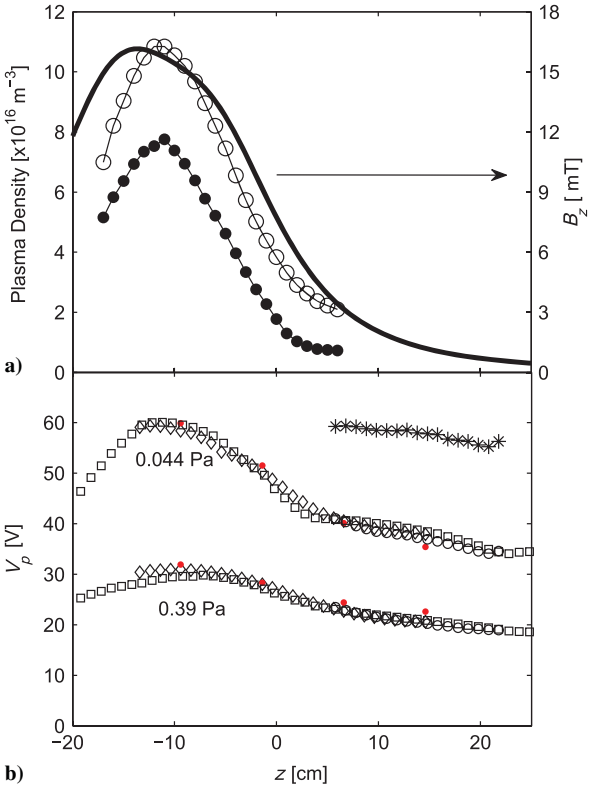


**Fig. 22 Graphs showing a) calculated magnetic field strength on axis (solid line) and axial plasma density for 0.044 Pa (0.33 mtorr, filled circles) and 0.39 Pa (2.92 mtorr, open circles), and b) plasma potential measurements made with the floating emissive probe method (open diamonds), the inflection point technique for emissive probes (closed circles), RFEA 1 (open squares), and RFEA 2 (open circles). The ion beam energy measured by RFEA 2 is also shown (stars). (Reproduced from Lafleur et al. [121], with permission from AIP Publishing.)**

where the field strength drops from 16 mT (160 G) to ~0.5 mT (5 G) [121]. The plasma source region was approximately in the range from −16 to −5 cm, resulting in a maximum density in that region followed by a density drop, as measured by a Langmuir probe. Figure 22b shows plasma potential measurements made with a variety of devices for two different neutral pressure cases. An emissive probe was used with both the floating point technique and the inflection point technique. Two different retarding field energy analyzers (RFEAs) were used to measure both the plasma potential and the ion beam energy. Notice that both emissive probe techniques accurately measured the plasma potential in the presence of a beam.

Gyergyek et al. [9] used a fluid model to describe the potential profile near an electron emitting surface in the presence of an electron beam. This analysis showed that a surface will float near the beam energy, not the plasma potential, when the fraction of beam electrons in the plasma is more than just a few percent. Similar results were found when analyzing a bi-Maxwellian plasma electron energy distribution, except that three values of the floating potential are also possible (two of which are stable) for certain fractions of the higher energy portion of the distribution [46,122,123]. Therefore, care must be taken when using the floating potential technique in a plasma with an electron beam. That technique should be validated against the inflection point technique, which can accurately measure the plasma potential even in the presence of a large electron beam [109].

### D. Temporal Resolution

Emissive probes can be used to make time-resolved measurements of the plasma potential much more simply than swept Langmuir probes when using the floating point in large emission because no voltage sweep is required [39,56,73]. With care, the time response can be reduced to 1 $\mu$s or less, though in many implementations the large resistors used to float the probe will slow the response time, as discussed in Sec. III.A.

Fujita and Yagura [39] modeled the plasma as a voltage source and resistor in series and determined the time response of a traditional large voltage divider of large resistance $R_M$ and small resistance $R_m$ to be

$$\tau_M = \frac{C_0 R_0 (R_M R_m)}{R_0 + R_M + R_m} \tag{26}$$

where $C_0$ is the probe stray capacitance and $R_0$ is the plasma resistance. Larger values of $(R_M + R_m)$ slow the response time, which was generally within an order of magnitude of 25 $\mu$s. By implementing an active circuit, Fujita and Yagura reduced the response time to better than 1 $\mu$s, limited only by their sampling resolution. Their circuit biases the probe near the plasma potential and iteratively adjusts toward it until the current across $R_M$ goes to zero. The circuit has the additional benefit of giving accurate potentials in low-density plasmas where a resistor only would skew the results.

The emissive probe circuit of Fig. 8 has reported similar time resolution using simpler passive components, but its time response has not yet been as robustly verified in a controlled time-varying plasma [43]. Fujita and Yagura [39] demonstrated their probe's response to an applied a step function potential using a biased grid in their test plasma, whereas the frequency response of the circuit in Fig. 8 was tested via a broadband chirp signal from 10 Hz to 1 MHz applied directly to the filament tip at atmosphere from a function generator. A Bode plot of the response showed unity gain up to 100 kHz ($\tau = 10$ $\mu$s) with slight resonances but otherwise good response out to 1 MHz ($\tau = 1$ $\mu$s), and the probe was used in the plume of a high-power Hall thruster.

Finally, Teii et al. [73] used a laser-heated floating emissive probe to resolve the plasma potential and extract electric fields in an RF capacitive discharge, demonstrating the ability to measure the electric field as a function of positive at a given phase in an RF cycle.

It has recently been demonstrated that the inflection point in the limit of zero emission technique can be used to make time-resolved plasma potential measurements [124]. It is possible to obtain time-resolved I-V traces by sweeping the probe bias faster than the plasma potential fluctuation, which is known as the fast-sweep method [40,125]. This method, however, requires carefully designed electronics and the measurements can be difficult to make. If the potential fluctuations are regular, the slow-sweep method can be used [126,127]. To perform the slow-sweep method, the probe current is measured as a function of time for a variety of probe biases. By transposing the data array, the I-V trace as a function of time can be obtained and the inflection point in the limit of zero emission technique executed in the normal way.

If temporal variations in the plasma potential are periodic, such as in an RF discharge where the plasma potential varies sinusoidally, a variation of the inflection point technique can be used to gain an understanding of the extent of the plasma potential variation. An experiment by Wang et al. [128] consisted of a multidipole plasma chamber with a grid immersed in the plasma that could be powered with an RF power supply. A filament discharge created a dc plasma over which an RF signal was applied by the grid. This configuration allowed the inflection point technique in a dc discharge to be compared with an RF discharge with the same temperature and density. Time-averaged emissive probe I-V traces for various amplitudes of RF voltage are shown in Fig. 23a [128]. Each point in the I-V trace should be measured with a collection time much longer than the RF period. Because typical RF periods are <1 $\mu$s, this condition can be achieved with a typical DAQ system and a circuit similar to the one shown in Fig. 12.

Differentiating the I-V trace (Fig. 23b) gives an indication of both the range of the plasma potential as well as the relative fraction of the RF period that the plasma spends at each potential. With a dc plasma (line a), the inflection point, which can be identified as the peak of the $dI/dV$ curve, occurs near the plasma potential (slightly below it). Increasing the RF amplitude significantly modifies the I-V trace so

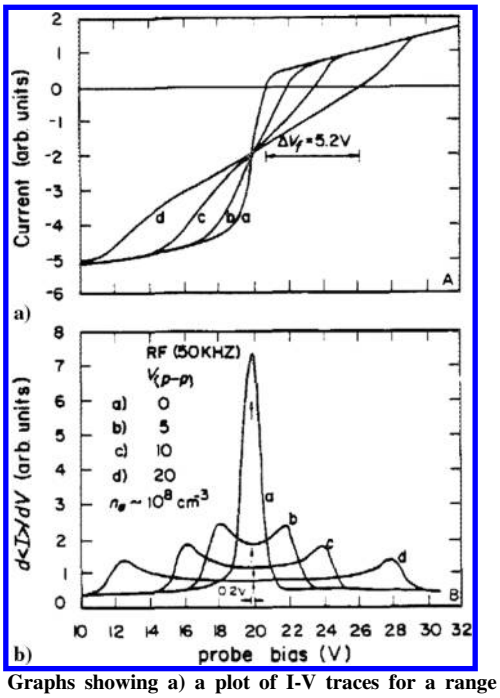


**Fig. 23 Graphs showing a) a plot of I-V traces for a range of RF amplitudes as indicated in Fig. 23b, and b) derivatives of the curves in Fig. 23a. (Reproduced from Wang et al. [128], with permission from AIP Publishing.)**

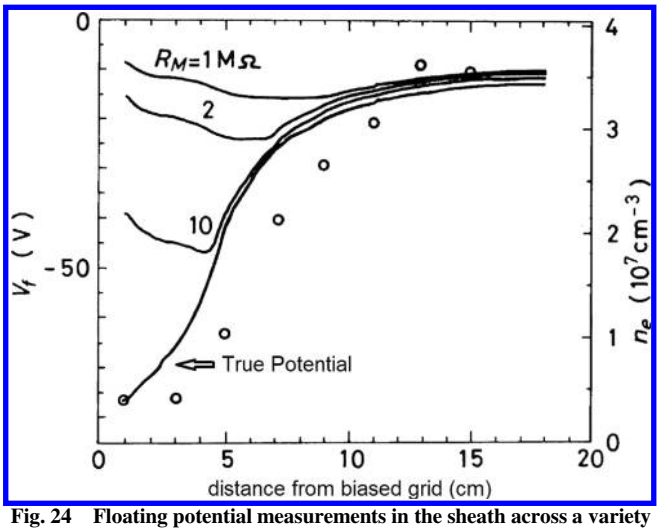


**Fig. 24 Floating potential measurements in the sheath across a variety of resistors. The open circles are the density measurements at various distances from the probe (Japan Society of Applied Physics, 1983).**

that the knee is less sharp because the plasma potential varies over the course of an RF period. The $dI/dV$ curve with RF fluctuations (lines b–d) can be interpreted as an approximate probability distribution (which is related to the EEDF [15]) of the plasma potential over the RF period [28,128]. In Fig. 23b, there are peaks in the $dI/dV$ curve at the plasma potential extremes because the potential fluctuation was sinusoidal and the plasma spends more time near the minimum and maximum potentials. An asymmetric $dI/dV$ curve, if the peak in line $d$ at 28 V was larger than the one at 12 V, for instance, would indicate that the plasma potential was spending more time near 28 V than any other potential. This can be caused by nonsinusoidal potential fluctuations [129].

When using the inflection point technique in an RF plasma, it is important for the emission current to be larger than the collected current. If the current is too small, then the inflection point features will not be resolvable. If the current is too large, then the emitted electrons can disrupt the plasma due to space-charge effects. Emission currents (and, therefore, filament temperatures) too high will decrease the peak resolution because the inflection point technique can only resolve to a factor of $T_w/e$ [128].

A time-averaged floating potential technique cannot be reliably used in an RF plasma [130]. Depending on the load resistor, the real impedance across which the probe current is measured, the floating potential may follow the average plasma potential, but could also vary with the RF voltage. The inflection point method (not in the limit of zero emission) is the preferable method because it can determine the fluctuations in the plasma potential when the trace is taken over a period much longer than the RF period.

### E. Sheaths

A common method of measuring the plasma potential using a Langmuir probe is by the knee of the I-V trace (the abrupt bend in the curve where electron saturation begins). Yamada and Murphree [88] showed that measuring the plasma potential in a sheath using that method does not give an accurate measurement with a planar Langmuir probe because it becomes a boundary in the sheath and disrupts the local space-charge of the sheath. Additionally, drifting ions and electrons in the sheath will shift the knee of the I-V trace for any probe geometry (planar, cylindrical, or spherical) and adversely affect potential measurements. Emissive probes, however, do not have this problem [88].

Though the floating point method can measure the potential in a sheath, it is limited by density. Fujita and Yagura [39] measured the floating potential using a resistor connected between ground and the emissive probe. They showed that, if the density in the sheath is too low, the emissive probe ceases to float near the plasma potential (see Fig. 24) [39]. The density at which the floating point method fails depends on the resistor across which the potential is measured. Smaller resistors lead to a larger limiting density. The true potential profile was measured using a high-impedance operational amplifier. Diebold et al. [65] compared the inflection point in the limit of zero emission method to the floating point method with a resistor and with an operational amplifier and found that the floating point method with a resistor failed close to the biased boundary, whereas the other two methods yielded expected results.

Wang and Hershkowitz [131] showed that, if the inflection point in the limit of zero emission method is used, the sheath/presheath boundary can easily be determined. For a probe to emit in the bulk (far from any surface), the probe bias must be below the plasma potential. This means that the inflection point of an emissive I-V trace will be below the plasma potential and approach it as the current is reduced to zero (see Fig. 25a) [131]. Conversely, in the ion sheath (a sheath in which the ion density is greater than the electron density, one with negative curvature), the inflection points are above the plasma potential because the emitted electron density affects the curvature of the potential in accordance with Poisson's equation (see Fig. 25b). Therefore, the position at which the inflection point does not depend on emission is the sheath/presheath boundary [131]. This is a useful criterion in multispecies plasmas where the sheath edge cannot be otherwise determined [132].

## VII. Which Method to Use?

The preceding may seem a daunting list of considerations for the new emissive probe user. Fortunately, a large body of work can be drawn upon to determine how to build and operate an emissive probe for a particular experiment. The references provided in this article can serve as a useful starting point and some general comments are subsequently provided on using emissive probes in various electric propulsion experiments.

Some design features are general for almost all electric propulsion applications. Any deviation from these recommendations will be specifically stated in the following sections. Thoriated tungsten is the preferred filament material because of its low work function and high melting point. A typical filament diameter is 0.0125 cm. The hairpin design is almost always used because it is more physically robust than the linear design and can better withstand the harsh environment of

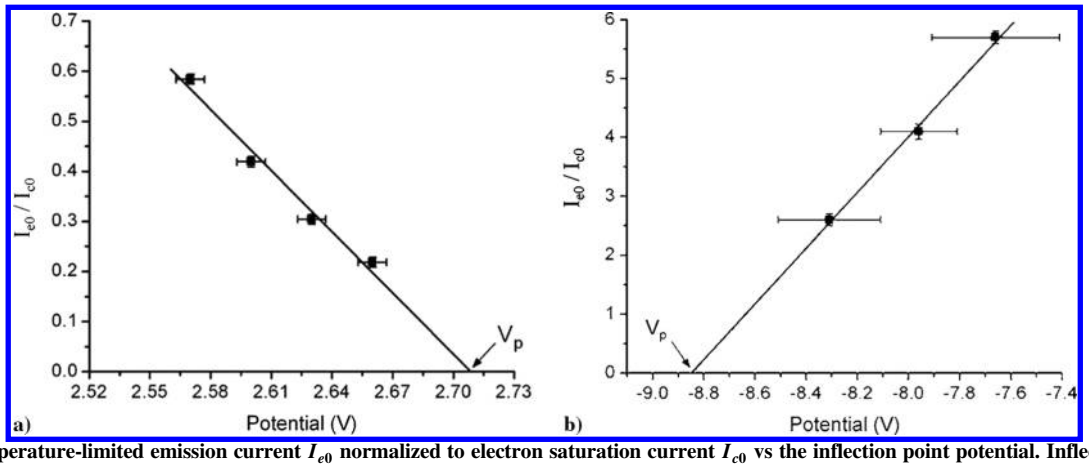


**Fig. 25 Temperature-limited emission current $I_{e0}$ normalized to electron saturation current $I_{e0}$ vs the inflection point potential. Inflection points at various emissions of an emissive probe in a) the bulk plasma, and b) an ion sheath. (Reproduced from Wang and Hershkowitz [131], with permission from AIP Publishing.)**



electric propulsion plasmas. Direct current Joule heating is the simplest way to heat the probe, only complicated by accounting for the potential drop across the filament. The floating point technique is most often used but should be calibrated versus the inflection point technique to ensure the sheath potential errors are minimal or can be accounted for.

### A. Plasma Plumes

In most thrusters, the plume is a comparatively low-density and low-temperature plasma, so any concerns about probe overheating from plasma current are minimal. The ion beam, however, can damage the emissive probe as a result of sputtering in a matter of hours, even if the probe is not in use. To maximize the lifetime of the probe, it should be removed from the plume when not in use. Using a larger filament diameter can extend the lifetime of the probe but requires more current to heat it. As the filament sputters away, the current required to heat the probe to emission decreases and the risk of probe failure increases.

### B. Hall Thruster Channel

The discharge in a Hall thruster channel has a high-energy density and probes in this plasma can be destroyed in a matter of seconds. A high-speed reciprocating motion stage is recommended to quickly insert the probe into the channel, take measurements, and remove the probe before it is destroyed [82]. If a high-speed motion table is used, it is important to ensure that the probe response time is shorter than the probe residence time in the plasma, otherwise, transients will affect the measurements.

Secondary electrons emitted from the ceramic probe shaft can significantly disrupt the discharge, making measurements less meaningful [7]. By coating the probe shaft in a material with low secondary electron emission, those effects can be greatly reduced.

### C. Ion Engine Discharge

Emissive probes are not often used in ion engine discharges because the potential structure is not a critical measurement to make. These discharges have densities, temperatures, and potentials similar to plasma processing devices, in which emissive probes have been used extensively [12]. Thinner filaments and lower heating currents can be used here because the plasma is less destructive.

### D. Helicon Thrusters

The floating potential method is most often used in helicon plasmas, though it is inherently a time-varying discharge. The potential varies over the RF period and the inflection point technique or a floating probe with a fast response time is needed to capture the fluctuations. With the highest magnetic fields, helicons are at the greatest risk of inducing probe distortion.

### E. Hollow Cathodes

Within 1 cm of a hollow cathode orifice, the plasma density can be as high as $1 \times 10^{15}$ cm$^{-3}$, so a high-speed translation stage is needed to prevent the probe from melting [133].

### F. Magnetoplasmadynamic Thrusters

MPD thruster plasmas have very high energy-densities and although Langmuir probes and triple probes have been used to measure the anode fall of these devices [134], emissive probes have not been used. High-speed translation would benefit measurements in MPDs just as in other situations where probe destruction is likely.

### G. Arcjets

Electric potential structures are not critical for understanding or evaluating arcjet operation, so emissive probes have not yet been used in those devices. They are a good candidate for self-emissive probes due to the high plasma density.

### H. Field Reversed Configuration Thrusters

Field reversed configuration thrusters are pulsed high-power thrusters (~100 kW) that are in development and have the potential to have a high-thrust-to-power ratio, specific impulse (~10,000 s), and high efficiency (~85%) [135]. This type of thruster is still highly experimental, so limited data on the plasma parameters are available. Because it is pulsed with pulse widths of 100 $\mu$s, any useful measurements need to be time resolved over even shorter timescales.

### I. Pulsed Plasma Thrusters

PPTs are inherently non-steady-state devices and require time-resolved measurements. Pulses are on the order of ~10 $\mu$s, and so megahertz-level probe frequency response is necessary [98].

### J. Electrospray Thrusters

Emissive probes have not been used in electrospray thrusters because the region of electric field typically has the same spatial scale as the filament itself, making the potential structure too small to resolve with a probe.

## VIII. Conclusion

Emissive probes have become an essential tool for diagnosing electric propulsion devices. By emitting electrons below the plasma potential but not above, they can be used to make measurements in a wide variety of conditions, making them well suited for electric propulsion plasmas which range from steady state to oscillatory, diffuse to dense, and cold to hot. Special care must be taken to account for the space-charge effects, which make interpreting emissive probe data more complex than it first appears. Yet, with

careful technique, emissive probes can provide insights into electric propulsion devices that cannot be obtained in any other way.

## Acknowledgments

This work was supported by U.S. Department of Energy (DE-FG02-97ER54437 and 3001346357), the Fusion Energy Sciences Fellowship Program administered by Oak Ridge Institute for Science and Education under a contract between the U.S. Department of Energy and the Oak Ridge Associated Universities, and the U.S. Air Force Office of Scientific Research. The authors would like to thank the referees for their thoughtful comments, which greatly improved this article.

## References

[1] Langmuir, I., "The Pressure Effect and Other Phenomena in Gaseous Discharges," *Journal of the Franklin Institute*, Vol. 196, No. 6, 1923, pp. 751–762. doi:10.1016/S0016-0032(23)90859-8

[2] Hobbs, G. D., and Wesson, J. A., "Heat Flow Through a Langmuir Sheath in the Presence of Electron Emission," *Plasma Physics*, Vol. 9, No. 1, 1967, pp. 85–87. doi:10.1088/0032-1028/9/1/410

[3] Raitses, Y., Staack, D., Smirnov, A., and Fisch, N. J., "Space Charge Saturated Sheath Regime and Electron Temperature Saturation in Hall Thrusters," *Physics of Plasmas*, Vol. 12, No. 7, 2005, Paper 073507. doi:10.1063/1.1944328

[4] Matsubara, A., Sugimoto, T., Shibuya, T., Kawamura, K., Sudo, S., and Sato, K., "Emissive Probe Measurement of Electron Temperature in Recombining Plasma Produced in the Linear Divertor Simulator TPD-II," *Journal of Nuclear Materials*, Vol. 313, March 2003, pp. 720–724. doi:10.1016/S0022-3115(02)01481-2

[5] Balan, P., et al., "Emissive Probe Measurements of Plasma Potential Fluctuations in the Edge Plasma Regions of Tokamaks," *Review of Scientific Instruments*, Vol. 74, No. 3, 2003, p. 1583. doi:10.1063/1.1527258

[6] Ionita, C., Balan, P., Schrittwieser, R., Figueiredo, H. F. C., Silva, C., Varandas, C. A. F., and Galvao, R. M. O., "Arrangement of Emissive and Cold Probes for Fluctuation and Reynolds Stress Measurements," *Review of Scientific Instruments*, Vol. 75, No. 10, 2004, pp. 4331–4333. doi:10.1063/1.1787582

[7] Staack, D., Raitses, Y., and Fisch, N. J., "Shielded Electrostatic Probe For Nonperturbing Plasma Measurements in Hall Thrusters," *Review of Scientific Instruments*, Vol. 75, No. 2, 2004, pp. 393–399. doi:10.1063/1.1634353

[8] Hershkowitz, N., "How Langmuir Probes Work," *Plasma Diagnostics*, edited by Auciello, O., and Flamm, D. L., Vol. 1, Academic Press, New York, 1989, pp. 113–183.

[9] Gyergyek, T., Kovacic, J., and Čerček, M., "A Fluid Model of the Sheath Formation in Front of an Electron Emitting Electrode with Space Charge Limited Emission Immersed in a Plasma that Contains a One-Dimensional Mono-Energetic Electron Beam," *Contributions to Plasma Physics*, Vol. 50, No. 2, 2010, pp. 121–134. doi:10.1002/ctpp.201010026

[10] Sheehan, J. P., Raitses, Y., Hershkowitz, N., Kaganovich, I., and Fisch, N. J., "A Comparison of Emissive Probe Techniques for Electric Potential Measurements in a Complex Plasma," *Physics of Plasmas*, Vol. 18, No. 7, 2011, Paper 073501. doi:10.1063/1.3601354

[11] Sun, X., Biloiu, C., Hardin, R., and Scime, E. E., "Parallel Velocity and Temperature of Argon Ions in an Expanding, Helicon Source Driven Plasma," *Plasma Sources Science and Technology*, Vol. 13, No. 3, 2004, pp. 359–370. doi:10.1088/0963-0252/13/3/001

[12] Sheehan, J. P., and Hershkowitz, N., "Emissive Probes," *Plasma Sources Science and Technology*, Vol. 20, No. 6, 2011, Paper 063001. doi:10.1088/0963-0252/20/6/063001

[13] Langmuir, I., and Compton, K. T., "Electrical Discharges in Gases Part II. Fundamental Phenomena in Electrical Discharges," *Reviews of Modern Physics*, Vol. 3, No. 2, 1931, pp. 191–257. doi:10.1103/RevModPhys.3.191

[14] Kemp, R. F., and Sellen, J. M., "Plasma Potential Measurements by Electron Emissive Probes," *Review of Scientific Instruments*, Vol. 37, No. 4, 1966, p. 455. doi:10.1063/1.1720213

[15] Godyak, V. A., and Demidov, V. I., "Probe Measurements of Electron-Energy Distributions in Plasmas: What Can We Measure and How Can We Achieve Reliable Results?" *Journal of Physics D: Applied Physics*, Vol. 44, No. 23, 2011, Paper 233001.

[16] Cohen, H. A., Sherman, C., Mullen, E. G., Huber, W. B., Masek, T. D., Sluder, R. B., Mizera, P. F., Schnauss, E. R., Adamo, R. C., and Nanevicz, J. E., "Design, Development, and Flight of a Spacecraft Charging Sounding Rocket Payload," U.S. Air Force Geophysics Lab., No. 19790015838, Hanscom AFB, MA, 1979.

[17] Mizera, P. F., Schnauss, E. R., Vandre, R., and Mullen, E. G., "Description and Charging Results from the RSPM," NASA Lewis Research Center Spacecraft Charging Technology, No. 19790015839, 1979.

[18] Bohm, D., "Minimum Ionic Kinetic Energy for a Stable Sheath," *Characteristics of Electrical Discharges in Magnetic Fields*, edited by Guthrie, A., and Wakerling, R. K., National Nuclear Energy Series, 1st ed., Manhattan Project Technical Section, Div. I, McGraw–Hill, New York, 1949, pp. 77–86.

[19] Mott-Smith, H. M., and Langmuir, I., "The Theory of Collectors in Gaseous Discharges," *Physical Review*, Vol. 28, No. 4, 1926, pp. 727–763. doi:10.1103/PhysRev.28.727

[20] Smith, J. R., Hershkowitz, N., and Coakley, P., "Inflection-Point Method of Interpreting Emissive Probe Characteristics," *Review of Scientific Instruments*, Vol. 50, No. 2, 1979, pp. 210–218. doi:10.1063/1.1135789

[21] Ibach, H., and Lüth, H., *Solid-State Physics: An Introduction to Principles of Materials Science*, 4th ed., Springer–Verlag, Berlin, 2009, p. 154.

[22] Crowell, C. R., "The Richardson Constant for Thermionic Emission in Schottky Barrier Diodes," *Solid-State Electronics*, Vol. 8, No. 4, 1965, pp. 395–399. doi:10.1016/0038-1101(65)90116-4

[23] Harbaugh, W. E., "Tungsten, Thoriated-Tungsten, and Thoria Emitters," *Electron Tube Design*, Radio Corp. of America, Harrison, NJ, 1962, pp. 90–98.

[24] Dorf, L., Raitses, Y., and Fisch, N. J., "Electrostatic Probe Apparatus for Measurements in the Near-Anode Region of Hall Thrusters," *Review of Scientific Instruments*, Vol. 75, No. 5, 2004, pp. 1255–1260. doi:10.1063/1.1710698

[25] Rozhansky, V. A., and Tsendin, L. D., *Transport Phenomena in Partially Ionized Plasma*, Taylor and Francis, London, 2001, pp. 88–90, Chap. 3.

[26] Takamura, S., Ohno, N., Ye, M. Y., and Kuwabara, T., "Space-Charge Limited Current from Plasma-Facing Material Surface," *Contributions to Plasma Physics*, Vol. 44, Nos. 13, 2004, pp. 126–137.

[27] Marek, A., Jilek, M., Pickova, I., Kudrna, P., Tichy, M., Schrittwieser, R., and Ionita, C., "Emissive Probe Diagnostics in Low Temperature Plasma—Effect of Space Charge and Variations of Electron Saturation Current," *Contributions to Plasma Physics*, Vol. 48, Nos. 5–7, 2008, pp. 491–496. doi:10.1002/ctpp.200810079

[28] Ye, M. Y., and Takamura, S., "Effect of Space-Charge Limited Emission on Measurements of Plasma Potential Using Emissive Probes," *Physics of Plasmas*, Vol. 7, No. 8, 2000, pp. 3457–3463. doi:10.1063/1.874210

[29] Hagino, Y., Ohno, N., Takamura, S., and Ye, M. Y., "Experimental Evaluation of Space Charge Limited Emission Current from Tungsten Surface in High Density Helium Plasma," *Journal of Nuclear Materials*, Vol. 313, March 2003, pp. 675–678. doi:10.1016/S0022-3115(02)01381-8

[30] Schrittwieser, R., et al., "Laser-Heated Emissive Plasma Probe," *Review of Scientific Instruments*, Vol. 79, No. 8, 2008, Paper 083508. doi:10.1063/1.2968114

[31] Fruchtman, A., Zoler, D., and Makrinich, G., "Potential of an Emissive Cylindrical Probe in Plasma," *Physical Review E: Statistical, Nonlinear, and Soft Matter Physics*, Vol. 84, No. 2, 2011, Paper 025402. doi:10.1103/PhysRevE.84.025402

[32] Allen, J. E., "Probe Theory—The Orbital Motion Approach," *Physica Scripta*, Vol. 45, No. 5, 1992, pp. 497–503. doi:10.1088/0031-8949/45/5/013

[33] Robertson, S., "The Electron Sheath Around an Emissive Wire in Vacuum," *IEEE Transactions on Plasma Science*, Vol. 40, No. 10, 2012, pp. 2678–2685. doi:10.1109/TPS.2012.2210915

[34] Reid, B. M., and Gallimore, A. D., "Plasma Potential Measurements in the Discharge Channel of a 6-kW Hall Thruster," *Joint Propulsion Conference*, AIAA Paper 2008-5185, 2008.

[35] Snyder, J. S., Goebel, D. M., Hofer, R. R., Polk, J. E., Wallace, N. C., and Simpson, H., "Performance Evaluation of the T6 Ion Engine," *46th Joint Propulsion Conference and Exhibit*, AIAA Paper 2010-7114, 2010.

[36] Staack, D., Raitses, Y., and Fisch, N. J., "Temperature Gradient in Hall Thrusters," *Applied Physics Letters*, Vol. 84, No. 16, 2004,

pp. 3028–3030.
doi:10.1063/1.1710732
[37] Haas, J. M., and Gallimore, A. D., "Internal Plasma Potential Profiles in a Laboratory-Model Hall Thruster," *Physics of Plasmas*, Vol. 8, No. 2, 2001, pp. 652–660.
doi:10.1063/1.1338535
[38] Bradley, J. W., Thompson, S., and Gonzalvo, Y. A., "Measurement of the Plasma Potential in a Magnetron Discharge and the Prediction of the Electron Drift Speeds," *Plasma Sources Science and Technology*, Vol. 10, No. 3, 2001, pp. 490–501.
doi:10.1088/0963-0252/10/3/314
[39] Fujita, H., and Yagura, S., "Measurements of Fast Time Evolutions of Plasma Potential Using Emissive Probe," *Japanese Journal of Applied Physics Part 1 — Regular Papers Short Notes and Review Papers*, Vol. 22, No. 1, 1983, pp. 148–151.
doi:10.1143/JJAP.22.148
[40] Lobbia, R. B., and Gallimore, A. D., "Temporal Limits of a Rapidly Swept Langmuir Probe," *Physics of Plasmas*, Vol. 17, No. 7, 2010, Paper 073502.
doi:10.1063/1.3449588
[41] Makowski, M. A., and Emmert, G. A., "New Method to Measure Plasma Potential with Emissive Probes," *Review of Scientific Instruments*, Vol. 54, No. 7, 1983, pp. 830–836.
doi:10.1063/1.1137486
[42] Fujita, H., Yagura, S., and Yamada, E., "An Influence of a Heating Voltage on an Emissive Probe Characteristic in a Plasma," *Journal of the Physical Society of Japan*, Vol. 50, No. 11, 1981, pp. 3759–3761.
doi:10.1143/JPSJ.50.3759
[43] McDonald, M. S., Liang, R., and Gallimore, A. D., "Practical Application of Wide Bandwidth Floating Emissive Probes and Wavelet Analysis to the X2 Nested Hall Thruster," *International Electric Propulsion Conference*, Electric Rocket Propulsion Soc. Paper 2013-352, 2013.
[44] Schwager, L. A., "Effects of Secondary and Thermionic Electron Emission on the Collector and Source Sheaths of a Finite Ion Temperature Plasma Using Kinetic Theory and Numerical Simulation," *Physics of Fluids B*, Vol. 5, No. 2, 1993, pp. 631–645.
doi:10.1063/1.860495
[45] Taylor, R. J., "A Large Double Plasma Device for Plasma Beam and Wave Studies," *Review of Scientific Instruments*, Vol. 43, No. 11, 1972, p. 1675.
doi:10.1063/1.1685522
[46] Gyergyek, T., and Čerček, M., "Potential Formation in a Bounded Two-Electron Temperature Plasma System with Floating Collector that Emits Electrons," *Czechoslovak Journal of Physics*, Vol. 54, No. 4, 2004, pp. 431–460.
doi:10.1023/B:CJOP.0000020583.09944.2f
[47] Annaratone, B. M., Counsell, G. F., Kawano, H., and Allen, J. E., "On the Use of Double Probes in RF Discharges," *Plasma Sources Science and Technology*, Vol. 1, No. 4, 1992, pp. 232–241.
doi:10.1088/0963-0252/1/4/002
[48] Castro, R. M., Cirino, G. A., Verdonck, P., Maciel, H. S., Massi, M., Pisani, M. B., and Mansano, R. D., "A Comparative Study of Single and Double Langmuir Probe Techniques for RF Plasma Characterization," *Contributions to Plasma Physics*, Vol. 39, No. 3, 1999, pp. 235–246.
[49] Swift, J. D., and Schwar, M. J. R., *Electrical Probes for Plasma Diagnostics*, Elsevier, London, 1969, pp. 220–245, Chap. 12.
[50] Lochte-Holtgreven, W., and Richter, J., *Plasma Diagnostics*, North-Holland, Amsterdam, 1968, pp. 668–731, Chap. 11.
[51] Bernstein, I. B., and Rabinowitz, I. N., "Theory of Electrostatic Probes in a Low-Density Plasma," *Physics of Fluids*, Vol. 2, No. 2, 1959, pp. 112–121.
doi:10.1063/1.1705900
[52] Laframboise, J. G., "Theory of Spherical and Cylindrical Langmuir Probes in a Collisionless, Maxwellian Plasma at Rest," Ph.D. Dissertation, Univ. of Toronto Libraries at Downsview, North York, ON, Canada, 1966.
[53] Steinbrüchel, C. ., "A New Method for Analyzing Langmuir Probe Data and the Determination of Ion Densities and Etch Yields in an Etching Plasma," *Journal of Vacuum Science and Technology A: Vacuum, Surfaces, and Films*, Vol. 8, No. 3, 1990, pp. 1663–1667.
doi:10.1116/1.576782
[54] Limpaecher, R., and MacKenzie, K. R., "Magnetic Multipole Containment of Large Uniform Collisionless Quiescent Plasmas," *Review of Scientific Instruments*, Vol. 44, No. 6, 1973, pp. 726–731.
doi:10.1063/1.1686231
[55] Sheehan, J. P., and Hershkowitz, N., "Negative Plasma Potential in a Multidipole Chamber with a Dielectric Coated Plasma Boundary," *Journal of Vacuum Science and Technology A: Vacuum, Surfaces, and Films*, Vol. 30, No. 3, 2012, Paper 031302.
doi:10.1116/1.4705514
[56] Godyak, V. A., and Piejak, R. B., "Probe Measurements of the Space Potential in a Radio-Frequency Discharge," *Journal of Applied Physics*, Vol. 68, No. 7, 1990, pp. 3157–3162.
doi:10.1063/1.346389
[57] Godyak, V. A., Piejak, R. B., and Alexandrovich, B. M., "Measurements of Electron Energy Distribution in Low-Pressure RF Discharges," *Plasma Sources Science and Technology*, Vol. 1, No. 1, 1992, pp. 36–58.
doi:10.1088/0963-0252/1/1/006
[58] Schwabedissen, A., Benck, E. C., and Roberts, J. R., "Langmuir Probe Measurements in an Inductively Coupled Plasma Source," *Physical Review E: Statistical, Nonlinear, and Soft Matter Physics*, Vol. 55, No. 3, 1997, pp. 3450–3459.
doi:10.1103/PhysRevE.55.3450
[59] Sobolewski, M. A., Olthoff, J. K., and Wang, Y. C., "Ion Energy Distributions and Sheath Voltages in a Radio-Frequency-Biased, Inductively Coupled, High-Density Plasma Reactor," *Journal of Applied Physics*, Vol. 85, No. 8, 1999, pp. 3966–3975.
doi:10.1063/1.370298
[60] Vender, D., and Boswell, R. W., "Electron Sheath Interaction in Capacitive Radiofrequency Plasmas," *Journal of Vacuum Science and Technology A: Vacuum, Surfaces, and Films*, Vol. 10, No. 4, 1992, pp. 1331–1338.
doi:10.1116/1.578248
[61] Chen, F. F., "Electric Probes," *Plasma Diagnostic Techniques*, edited by Huddlestone, R. H., and Leonard, S. L., Academic Press, New York, 1965, pp. 113–200, Chap. 4.
[62] Yao, W. E., Intrator, T., and Hershkowitz, N., "Direct Indication Technique of Plasma Potential with Differential Emissive Probe," *Review of Scientific Instruments*, Vol. 56, No. 4, 1985, pp. 519–524.
doi:10.1063/1.1138278
[63] Wang, E. Y., Hershkowitz, N., Diebold, D., Intrator, T., Majeski, R., Persing, H., Severn, G., Nelson, B., and Wen, Y. J., "Secondary-Electron Emission-Capacitive Probes for Plasma Potential Measurements in Plasmas with Hot-Electrons," *Journal of Applied Physics*, Vol. 61, No. 10, 1987, pp. 4786–4790.
doi:10.1063/1.338338
[64] Cho, M. H., Chan, C., Hershkowitz, N., and Intrator, T., "Measurement of Vacuum Space Potential by an Emissive Probe," *Review of Scientific Instruments*, Vol. 55, No. 4, 1984, pp. 631–632.
doi:10.1063/1.1137770
[65] Diebold, D., Hershkowitz, N., Bailey, A. D., Cho, M. H., and Intrator, T., "Emissive Probe Current Bias Method of Measuring DC Vacuum Potential," *Review of Scientific Instruments*, Vol. 59, No. 2, 1988, pp. 270–275.
doi:10.1063/1.1140239
[66] Mravlag, E., and Krumm, P., "Space Potential Measurements with a Continuously Emitting Probe," *Review of Scientific Instruments*, Vol. 61, No. 8, 1990, pp. 2164–2170.
doi:10.1063/1.1141384
[67] Kusaba, K., and Shindo, H., "A New Emissive-Probe Method for Electron Temperature Measurement in Radio-Frequency Plasmas," *Review of Scientific Instruments*, Vol. 78, No. 12, 2007, Paper 123503.
doi:10.1063/1.2821200
[68] Hershkowitz, N., Nelson, B., Pew, J., and Gates, D., "Self-Emissive Probes," *Review of Scientific Instruments*, Vol. 54, No. 1, 1983, pp. 29–34.
doi:10.1063/1.1137210
[69] Rohde, V., Laux, M., Bachmann, P., Herrmann, A., and Weinlich, M., "Direct Measurement of the Plasma Potential in the Edge of ASDEX Upgrade Using a Self Emitting Probe," *Journal of Nuclear Materials*, Vol. 241, Feb. 1997, pp. 712–715.
doi:10.1016/S0022-3115(97)80127-4
[70] Fink, M. A., Endler, M., and Klinger, T., "New Developments of Self-Emitting Electrostatic Probes for Use in High Temperature Plasmas," *Contributions to Plasma Physics*, Vol. 44, Nos. 7–8, 2004, pp. 668–676.
[71] Ono, S., and Teii, S., "Laser-Heated Emission of Electrons from a Carbon-Coated Metal-Surface and Its Application to the Emissive Probe Measurements," *Review of Scientific Instruments*, Vol. 50, No. 10, 1979, pp. 1264–1267.
doi:10.1063/1.1135693
[72] Mizumura, M., Uotsu, S., Matsumura, S., and Teii, S., "Probe System with Bias Compensation Using a Laser Heated Emissive Probe for RF Discharge Plasma Diagnostics," *Journal of Physics D: Applied Physics*, Vol. 25, No. 12, 1992, pp. 1744–1748.
doi:10.1088/0022-3727/25/12/009
[73] Teii, K., Mizumura, M., Matsumura, S., and Teii, S., "Time- and Space-Resolved Electric Potentials in a Parallel-Plate Radio-Frequency

Plasma," *Journal of Applied Physics*, Vol. 93, No. 10, 2003, pp. 5888–5892.
doi:10.1063/1.1568158

[74] Schrittwieser, R. W., Stärz, R., Ionita, C., Gstrein, R., Windisch, T., Grulke, O., and Klinger, T., "A Radially Movable Laser-Heated Emissive Probe," *Journal of Plasma Fusion Research*, Vol. 8, 2009, pp. 632–636, http://www.jspf.or.jp/JPFRS/.

[75] Ionita, C., et al., "The Use of Emissive Probes in Laboratory and Tokamak Plasmas," *Contributions to Plasma Physics*, Vol. 51, Nos. 2–3, 2011, pp. 264–270.
doi:10.1002/ctpp.201000067

[76] Ionita, C., Balan, P., Windisch, T., Brandt, C., Grulke, O., Klinger, T., and Schrittwieser, R., "New Results on a Laser-Heated Emissive Probe," *Contributions to Plasma Physics*, Vol. 48, Nos. 5–7, 2008, pp. 453–460.
doi:10.1002/ctpp.200810073

[77] Schrittwieser, R., Sarma, A., Amarandei, G., Ionita, C., Klinger, T., Grulke, O., Vogelsang, A., and Windisch, T., "Results of Direct Measurements of the Plasma Potential Using a Laser-Heated Emissive Probe," Vol. T123, Royal Swedish Academy of Sciences, Stockholm, pp. 94–98.

[78] Amarandei, G., Dimitriu, D. G., Sarma, A. K., Balan, P. C., Klinger, T., Grulke, O., Ionita, C., and Schrittwieser, R., "Studies on Suitable Materials for a Laser-Heated Electron-Emissive Plasma Probe," *Romanian Journal of Physics*, Vol. 53, Nos. 1–2, 2008, pp. 311–316.

[79] Lassner, E., and Schubert, W.-D., *Tungsten: Properties, Chemistry, Technology of the Element, Alloys, and Chemical Compounds*, Kluwer Academic, Norwell, MA, 1999, pp. 40–42.

[80] Langmuir, I., "The Electron Emission from Thoriated Tungsten Filaments," *Physical Review*, Vol. 22, No. 4, 1923, pp. 357–398.
doi:10.1103/PhysRev.22.357

[81] Schrittwieser, R., et al., "Measurements with an Emissive Probe in the CASTOR Tokamak," *Plasma Physics and Controlled Fusion*, Vol. 44, No. 5, 2002, pp. 567–578.
doi:10.1088/0741-3335/44/5/305

[82] Haas, J. M., Gallimore, A. D., McFall, K., and Spanjers, G., "Development of a High-Speed, Reciprocating Electrostatic Probe System for Hall Thruster Interrogation," *Review of Scientific Instruments*, Vol. 71, No. 11, 2000, pp. 4131–4138.
doi:10.1063/1.1318921

[83] Tartz, M., Heyn, T., Bundesmann, C., Zimmermann, C., and Neumann, H., "Sputter Yields of Mo, Ti, W, Al, Ag Under Xenon Ion Incidence," *European Physical Journal D*, Vol. 61, No. 3, 2011, pp. 587–592.
doi:10.1140/epjd/e2010-10553-8

[84] Stuart, R. V., and Wehner, G. K., "Sputtering Yields at Very Low Bombarding Ion Energies," *Journal of Applied Physics*, Vol. 33, No. 7, 1962, p. 2345.
doi:10.1063/1.1728959

[85] Rosenberg, D., and Wehner, G. K., "Sputtering Yields for Low Energy He+, Kr+, and Xe+ Ion Bombardment," *Journal of Applied Physics*, Vol. 33, No. 5, 1962, p. 1842.
doi:10.1063/1.1728843

[86] Wang, X., Howes, C. T., Horanyi, M., and Robertson, S., "Effect of Filament Supports on Emissive Probe Measurements," *Review of Scientific Instruments*, Vol. 84, No. 1, 2013, Paper 013506.

[87] Petrunin, I. E., and Grzhimal'skii, L. L., "Interaction of Tungsten with Copper, Manganese, Silver, and Tin," *Metal Science and Heat Treatment*, Vol. 11, No. 1, 1969, pp. 24–26.
doi:10.1007/BF00655167

[88] Yamada, H., and Murphree, D. L., "Electrostatic Probe Measurements in a Collisionless Plasma Sheath," *Physics of Fluids*, Vol. 14, No. 6, 1971, p. 1120.
doi:10.1063/1.1693574

[89] Motley, R. W., "Hot-Probe Measurements of Space Potential Oscillations in a Plasma," *Journal of Applied Physics*, Vol. 43, No. 9, 1972, p. 3711.
doi:10.1063/1.1661795

[90] Iizuka, S., Michelsen, P., Rasmussen, J. J., Schrittwieser, R., Hatakeyama, R., Saeki, K., and Sato, N., "A Method for Measuring Fast Time Evolutions of the Plasma Potential by Means of a Simple Emissive Probe," *Journal of Physics E: Scientific Instruments*, Vol. 14, No. 11, 1981, pp. 1291–1295.
doi:10.1088/0022-3735/14/11/017

[91] Siebenforcher, A., and Schrittwieser, R., "A New Simple Emissive Probe," *Review of Scientific Instruments*, Vol. 67, No. 3, 1996, pp. 849–850.
doi:10.1063/1.1146823

[92] Auweter-Kurtz, M., Golz, T., Habiger, H., Hammer, F., Kurtz, H., Riehle, M., and Sleziona, C., "High-Power Hydrogen Arcjet Thrusters," *Journal of Propulsion and Power*, Vol. 14, No. 5, 1998, pp. 764–773.
doi:10.2514/2.5339

[93] Reid, B. M., and Gallimore, A. D., "Langmuir Probe Measurements in the Discharge Channel of a 6-kW Hall Thruster," *Joint Propulsion Conference*, AIAA Paper 2008-4920, 2008.

[94] Sekerak, M. J., McDonald, M. S., Hofer, R. R., and Gallimore, A. D., "Hall Thruster Plume Measurements from High-Speed Dual Langmuir Probes with Ion Saturation Reference," *IEEE Aerospace Conference*, Inst. of Electrical and Electronics Engineers Paper 2013-2129, 2013.

[95] West, M. D., Charles, C., and Boswell, R. W., "Testing a Helicon Double Layer Thruster Immersed in a Space-Simulation Chamber," *Journal of Propulsion and Power*, Vol. 24, No. 1, 2008, pp. 134–141.
doi:10.2514/1.31414

[96] Foster, J. E., Soulas, G. C., and Patterson, M. J., "Plume and Discharge Plasma Measurements of an NSTAR-Type Ion Thruster," *Joint Propulsion Conference*, AIAA Paper 2000-3812, 2000.

[97] Kubota, K., Funaki, I., and Okuno, Y., "Comparison of Simulated Plasma Flow Field in a Two-Dimensional Magnetoplasmadynamic Thruster with Experimental Data," *IEEE Transactions on Plasma Science*, Vol. 37, No. 12, 2009, pp. 2390–2398.
doi:10.1109/TPS.2009.2032913

[98] Eckman, R., Byrne, L., Gatsonis, N. A., and Pencil, E. J., "Triple Langmuir Probe Measurements in the Plume of a Pulsed Plasma Thruster," *Journal of Propulsion and Power*, Vol. 17, No. 4, 2001, pp. 762–771.
doi:10.2514/2.5831

[99] Nawaz, A., Lau, M., Herdrich, G., and Auweter-Kurtz, M., "Investigation of the Magnetic Field in a Pulsed Plasma Thruster," *AIAA Journal*, Vol. 46, No. 11, 2008, pp. 2881–2889.
doi:10.2514/1.37161

[100] Riemann, K. U., "The Bohm Criterion and Sheath Formation," *Journal of Physics D: Applied Physics*, Vol. 24, No. 4, 1991, pp. 493–518.
doi:10.1088/0022-3727/24/4/001

[101] Raitses, Y., Staack, D., Keidar, M., and Fisch, N. J., "Electron-Wall Interaction in Hall Thrusters," *Physics of Plasmas*, Vol. 12, No. 5, 2005, Paper 057104.
doi:10.1063/1.1891747

[102] Meyer, J. A., Kim, G. H., Goeckner, M. J., and Hershkowitz, N., "Measurements of the Presheath in an Electron Cyclotron Resonance Etching Device," *Plasma Sources Science and Technology*, Vol. 1, No. 3, 1992, pp. 147–150.
doi:10.1088/0963-0252/1/3/001

[103] Raitses, Y., Kaganovich, I. D., Khrabrov, A., Sydorenko, D., Fisch, N. J., and Smolyakov, A., "Effect of Secondary Electron Emission on Electron Cross-Field Current in ExB Discharges," *IEEE Transactions on Plasma Science*, Vol. 39, No. 4, 2011, pp. 995–1006.
doi:10.1109/TPS.2011.2109403

[104] Kaganovich, I. D., Raitses, Y., Sydorenko, D., and Smolyakov, A., "Kinetic Effects in a Hall Thruster Discharge," *Physics of Plasmas*, Vol. 14, No. 5, 2007, Paper 057104.
doi:10.1063/1.2709865

[105] Cartier, S. L., and Merlino, R. L., "Anode-Type Double-Layers in a Nonuniform Magnetic-Field," *Physics of Fluids*, Vol. 30, No. 8, 1987, pp. 2549–2560.
doi:10.1063/1.866093

[106] Pedersen, T. S., Kremer, J. P., Lefrancois, R. G., Marksteiner, Q., Pomphrey, N., Reiersen, W., Dahlgren, F., and Sarasola, X., "Construction and Initial Operation of the Columbia Nonneutral Torus," *Fusion Science and Technology*, Vol. 50, No. 3, 2006, pp. 372–381.

[107] Skoro, G. P., Bennett, J. R. J., Edgecock, T. R., Gray, S. A., McFarland, A. J., Booth, C. N., Rodgers, K. J., and Back, J. J., "Dynamic Young's Moduli of Tungsten and Tantalum at High Temperature and Stress," *Journal of Nuclear Materials*, Vol. 409, No. 1, 2011, pp. 40–46.
doi:10.1016/j.jnucmat.2010.12.222

[108] Longmier, B. W., Squire, J. P., Olsen, C. S., Cassady, L. D., Ballenger, M. G., Carter, M. D., Ilin, A. V., Glover, T. W., McCaskill, G. E., Chang Díaz, F. R., and Bering, E. A., "Improved Efficiency and Throttling Range of the VX-200 Magnetoplasma Thruster," *Journal of Propulsion and Power*, Vol. 30, No. 1, 2014, pp. 123–132.
doi:10.2514/1.B34801

[109] Coakley, P., and Hershkowitz, N., "Laboratory Double-Layers," *Physics of Fluids*, Vol. 22, No. 6, 1979, pp. 1171–1181.
doi:10.1063/1.862719

[110] Gyergyek, T., and Čerček, M., "A Fluid Model of the Current-Voltage Characteristics of an Electron Emitting Electrode Immersed in a Two Electron Temperature Plasma," *European Physical Journal D*, Vol. 42, No. 3, 2007, pp. 441–454.
doi:10.1140/epjd/e2007-00132-7

[111] Ruiz, M., Urdampilleta, I., del Cura, J. M., Ahedo, E., and Navarro-Cavalle, J., "Space Missions Potentially Benefit or Enabled by the Prospective Use of Helicon Plasma Thrusters," *International Electric Propulsion Conference*, Electric Rocket Propulsion Soc. Paper 2013-273, 2013.

[112] Shinohara, S., et al., "High-Density Helicon Plasma Sources: Basics and Applications to Electrodeless Electric Propulsion," *Transactions of Fusion Science and Technology*, Vol. 63, No. 1T, 2013, pp. 164–167.

[113] Takahashi, K., et al., "Direct Thrust Measurement of a Permanent Magnet Helicon Double Layer Thruster," *Applied Physics Letters*, Vol. 98, No. 14, 2011, Paper 141503. doi:10.1063/1.3577608

[114] Shinohara, S., Nishida, H., Tanikawa, T., Hada, T., Funaki, I., and Shamrai, K. P., "Development of Electrodeless Plasma Thrusters with High-Density Helicon Plasma Sources," *IEEE Transactions on Plasma Science*, Vol. 42, No. 5, 2014, pp. 1245–1254. doi:10.1109/TPS.2014.2313633

[115] Sheehan, J. P., Longmier, B. W., Reese, I., and Collard, T., "New Low-Power Plasma Thruster for Nanosatellites," *AIAA Propulsion and Energy Forum and Exposition*, AIAA Paper 2014-3914, 2014.

[116] Charles, C., and Boswell, R., "Current-Free Double-Layer Formation in a High-Density Helicon Discharge," *Applied Physics Letters*, Vol. 82, No. 9, 2003, pp. 1356–1358. doi:10.1063/1.1557319

[117] Sahu, B. B., Tarey, R. D., and Ganguli, A., "Experimental Investigation of Current Free Double Layers in Helicon Plasmas," *Physics of Plasmas*, Vol. 21, No. 2, 2014, Paper 023504. doi:10.1063/1.4864651

[118] Sheehan, J. P., et al., "Temperature Gradients Due to Adiabatic Plasma Expansion in a Magnetic Nozzle," *Plasma Sources Science and Technology*, Vol. 23, No. 4, 2014, Paper 045014. doi:10.1088/0963-0252/23/4/045014

[119] Fruchtman, A., "Electric Field in a Double Layer and the Imparted Momentum," *Physical Review Letters*, Vol. 96, No. 6, 2006, Paper 065002. doi:10.1103/PhysRevLett.96.065002

[120] Takahashi, K., Lafleur, T., Charles, C., Alexander, P., and Boswell, R. W., "Electron Diamagnetic Effect on Axial Force in an Expanding Plasma: Experiments and Theory," *Physical Review Letters*, Vol. 107, No. 23, 2011, Paper 235001. doi:10.1103/PhysRevLett.107.235001

[121] Lafleur, T., Charles, C., and Boswell, R. W., "Detailed Plasma Potential Measurements in a Radio-Frequency Expanding Plasma Obtained from Various Electrostatic Probes," *Physics of Plasmas*, Vol. 16, No. 4, 2009, Paper 044510. doi:10.1063/1.3125314

[122] Gyergyek, T., and Čerček, M., "Fluid Model of a Sheath Formed in Front of an Electron Emitting Electrode Immersed in a Plasma with Two Electron Temperatures," *Contributions to Plasma Physics*, Vol. 45, No. 2, 2005, pp. 89–110.

[123] Nam, C. H., Hershkowitz, N., Cho, M. H., Intrator, T., and Diebold, D., "Multiple Valued Floating Potentials of Langmuir Probes," *Journal of Applied Physics*, Vol. 63, No. 12, 1988, pp. 5674–5677. doi:10.1063/1.340301

[124] Sheehan, J. P., Barnat, E. V., Weatherford, B. R., Kaganovich, I. D., and Hershkowitz, N., "Emissive Sheath Measurements in the Afterglow of a Radio Frequency Plasma," *Physics of Plasmas*, Vol. 21, No. 1, 2014, Paper 013510. doi:10.1063/1.4861888

[125] Schubert, M., Endler, M., and Thomsen, H., "Spatiotemporal Temperature Fluctuation Measurements by Means of a Fast Swept Langmuir Probe Array," *Review of Scientific Instruments*, Vol. 78, No. 5, 2007, Paper 053505. doi:10.1063/1.2740785

[126] Maresca, A., Orlov, K., and Kortshagen, U., "Experimental Study of Diffusive Cooling of Electrons in a Pulsed Inductively Coupled Plasma," *Physical Review E: Statistical, Nonlinear, and Soft Matter Physics*, Vol. 65, No. 5, 2002, Paper 056405. doi:10.1103/PhysRevE.65.056405

[127] Gudmundsson, J. T., Alami, J., and Helmersson, U., "Spatial and Temporal Behavior of the Plasma Parameters in a Pulsed Magnetron Discharge," *Surface and Coatings Technology*, Vol. 161, Nos. 2–3, 2002, pp. 249–256. doi:10.1016/S0257-8972(02)00518-2

[128] Wang, E. Y., Hershkowitz, N., Intrator, T., and Forest, C., "Techniques for Using Emitting Probes for Potential Measurement in RF Plasmas," *Review of Scientific Instruments*, Vol. 57, No. 10, 1986, pp. 2425–2431. doi:10.1063/1.1139088

[129] Wiebold, M., Sung, Y.-T., and Scharer, J. E., "Ion Acceleration in a Helicon Source Due to the Self-Bias Effect," *Physics of Plasmas*, Vol. 19, No. 5, 2012, Paper 053503. doi:10.1063/1.4714605

[130] Bousselin, G., Lemoine, N., Cavalier, J., Heuraux, S., and Bonhomme, G., "Note: On the Measurement of Plasma Potential Fluctuations Using Emissive Probes," *Review of Scientific Instruments*, Vol. 85, No. 5, 2014, Paper 056102. doi:10.1063/1.4875585

[131] Wang, X., and Hershkowitz, N., "Simple Way to Determine the Edge of an Electron-Free Sheath with an Emissive Probe," *Review of Scientific Instruments*, Vol. 77, No. 4, 2006, Paper 043507. doi:10.1063/1.2195103

[132] Lee, D., Severn, G., Oksuz, L., and Hershkowitz, N., "Laser-Induced Fluorescence Measurements of Argon Ion Velocities Near the Sheath Boundary of an Argon-Xenon Plasma," *Journal of Physics D: Applied Physics*, Vol. 39, No. 24, 2006, pp. 5230–5235. doi:10.1088/0022-3727/39/24/020

[133] Jameson, K. K., Goebel, D. M., and Watkins, R. M., "Hollow Cathode and Thruster Discharge Chamber Plasma Measurements Using High-Speed Scanning Probes," *International Electric Propulsion Conference*, Electric Rocket Propulsion Soc. Paper 2005-269, 2005.

[134] Gallimore, A. D., Kelly, A. J., and Jahn, R. G., "Anode Power Deposition in Magnetoplasmadynamic Thrusters," *Journal of Propulsion and Power*, Vol. 9, No. 3, 1993, pp. 361–368. doi:10.2514/3.23630

[135] Slough, J., Kirtley, D., and Weber, T., "Pulsed Plasmoid Propulsion: The ELF Thruster," *International Electric Propulsion Conference*, Electric Rocket Propulsion Soc. Paper 2009-265, 2009.

J. Blandino
*Associate Editor*

**This article has been cited by:**


1. Igor Levchenko, Kateryna Bazaka, Yongjie Ding, Yevgeny Raitses, Stéphane Mazouffre, Torsten Henning, Peter J. Klar, Shunjiro Shinohara, Jochen Schein, Laurent Garrigues, Minkwan Kim, Dan Lev, Francesco Taccogna, Rod W. Boswell, Christine Charles, Hiroyuki Koizumi, Yan Shen, Carsten Scharlemann, Michael Keidar, Shuyan Xu. 2018. Space micropropulsion systems for Cubesats and small satellites: From proximate targets to furthermost frontiers. *Applied Physics Reviews* **5**:1, 011104. [Crossref]
2. Dan R. Lev, Gal Alon. 2018. Operation of a Hollow Cathode Neutralizer for Sub-100-W Hall and Ion Thrusters. *IEEE Transactions on Plasma Science* **46**:2, 311-318. [Crossref]
3. Xin Chen, Gonzalo Sánchez-Arriaga. 2018. Current-Voltage and Floating-Potential characteristics of cylindrical emissive probes from a full-kinetic model based on the orbital motion theory. *Journal of Physics: Conference Series* **958**, 012001. [Crossref]
4. S. J. Doyle, P. R. Salvador, K. G. Xu. 2017. Flame exposure time on Langmuir probe degradation, ion density, and thermionic emission for flame temperature. *Review of Scientific Instruments* **88**:11, 113503. [Crossref]
5. G. Sanchez-Arriaga. 2017. Kinetic features of collisionless sheaths around polarized cylindrical emitters from the orbital motion theory. *Physics of Plasmas* **24**:10, 103515. [Crossref]